Chapter

5

Dielectric Relaxation Study (DRS) and Electrochemical Impedance Spectroscopy (EIS) of Binary Mixtures (n-Octanol+ N, N-Dimethylformamide)

Contents

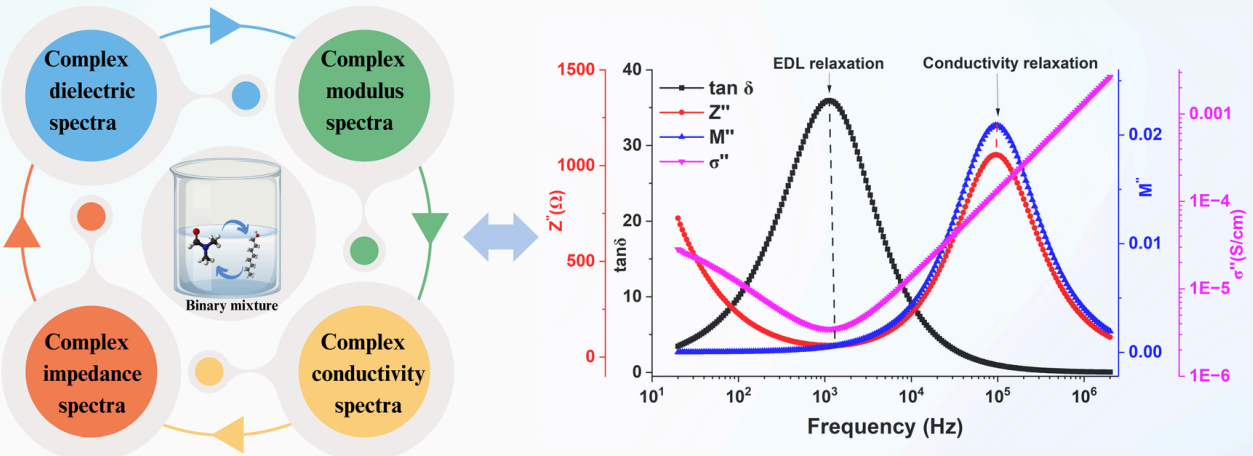

5.1 Introduction

The previous chapter presented findings from the dielectric relaxation spectroscopy analysis of binary mixtures of n-Hexanol and N, N-Dimethylformamide (DMF) over a broad frequency range. This investigation identified distinct relaxation processes, including electrode polarization and ionic conductivity relaxation mechanisms in the low-frequency range (20 Hz to 2 MHz) and dielectric relaxation occurring in the microwave frequency range (200 MHz to 20 GHz). The static permittivity of the studied system revealed details about hydrogen bonding and dipole-dipole interactions among the molecular species in the liquid mixtures. Furthermore, the microwave dielectric relaxation (MDR) (200 MHz to 20 GHz) of the binary system provided qualitative insights into molecular interactions, including the nature of hydrogen-bond linkages, the hindrance forces encountered by the molecules, and their orientation within the liquid mixtures. As a continuation of this work, a systematic investigation was carried out to understand the molecular interactions between n-Octanol and N, N-Dimethylformamide (DMF) using dielectric relaxation spectroscopy (DRS) over a broad frequency range. In this study, DMF serves as the common component in the binary systems n-Hexanol+DMF and n-Octanol+DMF, with the other component being alcohols of differing chain lengths. An analysis of the dielectric relaxation spectroscopy (DRS) data for both systems will offer deeper insights into the molecular interactions among the species within the two systems. The longer-chain alcohol, n-octanol, has been recognized as a biofuel candidate derived from biomass-derived platform chemicals [1]. Primary alcohols of medium chain length are crucial industrial products, serving as valuable compounds for detergent and surfactant production, as well as in perfumery and flavor applications. Particularly, 1-octanol holds significance and is employed in synthesizing 1-octene, a key co-monomer in polyethylene production and petrochemical processes [2]. This contrast provides an intriguing opportunity to explore how different polar solvent environments influence the molecular interactions of DMF with its co-solvent under varying conditions of concentration and temperature.

In this chapter, complex permittivity spectra ($\varepsilon^*(f)$) of binary mixtures (n-Octanol with N, N- Dimethylformamide) of various concentrations in the frequency range of 20 Hz to 2 MHz were determined using precision LCR meter at temperature 293.15 K, 303.15 K and 313.15 K. The complex impedance spectra ($Z^*(f)$), complex conductivity spectra ($\sigma^*(f)$), loss tangent ($\tan \delta$) and complex modulus spectra ($M^*(f)$) were determined

from the complex permittivity spectra (ε*(f)). Different relaxation times such as electrode polarization relaxation time (τ_{EP}), relaxation time(τ_{EP}'), and ionic conduction relaxation time (τ_σ) were calculated with the help of different dielectric and electrical mechanisms. A three-element equivalent circuit model was used to fit the complex impedance data. The fitting provided the values of various circuit elements representing various electrical processes occurring in the capacitive measurement cell under the influence of an applied ac field. The Bode plot presentation of the complex impedance data confirmed the values of various circuit elements determined using the fitting process. Furthermore, the complex permittivity spectra of binary mixtures of n-Octanol and DMF at varying concentrations (0.0 →1.0) were analyzed in the microwave frequency range (200 MHz to 20 GHz) across different temperatures (293.15 K,303.15 K and 313.15 K). The frequency-dependent microwave complex permittivity data were fitted to the Cole-Cole (CC) dielectric relaxation model using the complex nonlinear least squares (CNLS) fitting technique. The resulting dielectric relaxation times were analyzed within the framework of the wait-and-switch model. The obtained dielectric spectra are carefully analyzed using the Cole-Cole model to extract important dielectric properties, such as the dielectric relaxation strength (Δε) static dielectric constant (ε_0) and relaxation time (τ_d). The analysis of dielectric relaxation times for both associative and non-associative mixture solutions has been extensively studied using this model [3-8], which was originally proposed for alcohols by Sagal [9]. From the measured values, excess static permittivity $(\varepsilon_0)^E$ and excess inverse relaxation time $(1/\tau d)^E$ were calculated and fitted to the Redlich-Kister equation [10]. The effective correction factor (g^{eff}) and the corrective correlation factor (g^f) were determined using the modified Kirkwood equations (3.16 and 3.17) [11], with dipole moments of 1.60 D for n-Octanol and 3.86 D for N, N-Dimethylformamide (DMF) [12]. Additionally, experimental static permittivity data were analyzed using the modified Bruggeman equation to compute the Bruggeman factor (F_B) [13]. The excess parameters, Kirkwood correlation factors, and Bruggeman factor collectively provide insights into molecular interactions and orientation behavior under the influence of an applied static electric field.

5.2 Materials and Experimental methods

n-Octanol (synthesis grade) and N, N-Dimethylformamide (DMF) (AR grade) were obtained from Loba Chemie (India) and used without further purification. Binary mixtures of n-Octanol and DMF were prepared in hermetically sealed glass vials across

eleven volume concentrations, covering the entire composition range (X_1 = 0.0 to X_1 = 1.0), and were studied at various temperatures (293.15 K to 313.15 K). The volume fraction was converted to the mole fraction of n-Octanol (X_1) using Equation 3.1 [11]. Details of the experimental methods and setup used to determine relative dielectric function (ε*(f)) (using LCR and VNA) of the liquid samples is explained in Chapter 3. The experimental values of static permittivity (ε_0) for both pure compounds, n-Octanol and DMF, at different temperatures are presented in Table 5.1. To verify the purity of the compounds used in this study, these experimental values were compared with corresponding literature values in the same table. The experimental ε_0 values for the pure compounds show good agreement with the literature data [14-19].

Table 5.1 Comparison of static permittivity (ε_0) of pure compounds (n-Octanol and DMF) with literature data at different temperatures.

		Temperatures (K)		
Compounds	**Static Permittivity (ε_0)**	**293.15**	**303.15**	**313.15**
n-Octanol	Experimental	9.28	8.98	8.49
	Literature	10.08 [14]	9.01 [15]	8.52 [16]
DMF	Experimental	37.00	36.22	34.75
	Literature	37.69 [17]	36.65 [18]	35.09 [19]

5.3 Results and Discussion

- The results and discussion section is organized into two main parts.
  - I. Dielectric spectroscopy in the lower Frequency Range 20 Hz to 2 MHz (Using LCR Study).
  - II. Dielectric relaxation spectroscopy in the Higher Frequency Range 200 MHz to 20 GHz (Using VNA Study).

5.3.1 Dielectric spectroscopy in the lower Frequency Range 20 Hz to 2 MHz.

5.3.1.1 Complex Dielectric Spectra

Figure 5.1 (a), (b) and (c) show frequency dependent variation of real ε′(f) and imaginary ε′′(f) part of binary mixtures of n-Octanol with DMF and their concentration range X_A = 0.0 to X_A = 1.0 at different temperatures (293.15 K, 303.15 K and 313.15 K). Figure 5.1 shows that the permittivity spectra are divided into two different regions, in higher frequency region (It is independent of frequency) and lower frequency regions (It depends upon the frequency). In the higher frequency region below 10^4 Hz, the real

part of permittivity spectra (ε′(f)) is independent of the frequency, and it attenuates to the steady region. It is observed in the lower frequency region below 10^4 Hz, real ε′(f) part value increase with increase in the volume fraction of DMF.

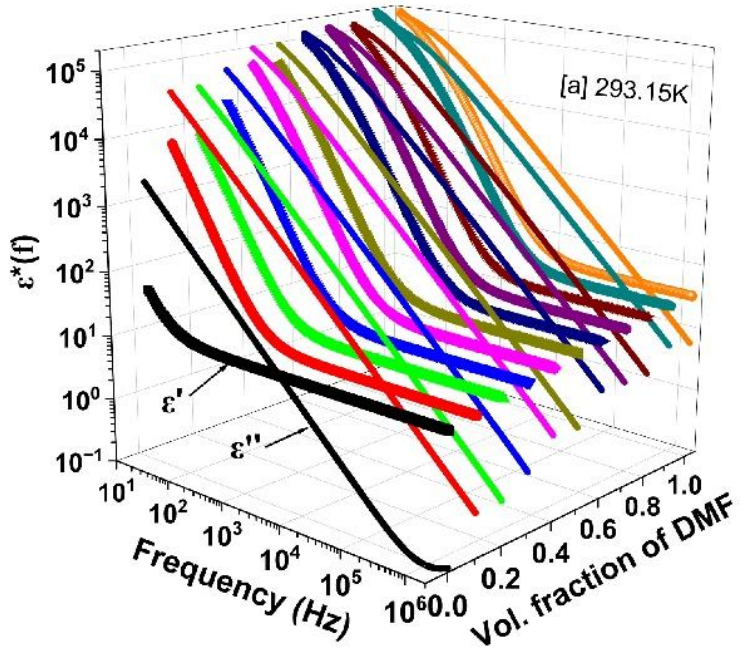

Fig. 5.1 (A) Variation of complex dielectric function ε*(f) against volume fraction of DMF in binary mixtures of all concentration range X_A = 0.0 to X_A= 1.0 at 293.15 K.

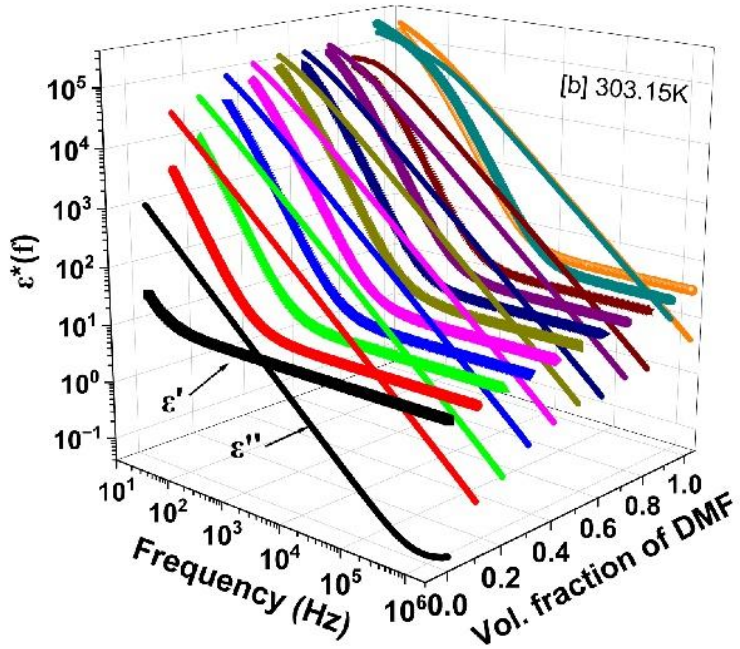

Fig. 5.1 (B) Variation of complex dielectric function ε*(f) against volume fraction of DMF in binary mixtures of all concentration range X_A = 0.0 to X_A= 1.0 at 303.15 K.

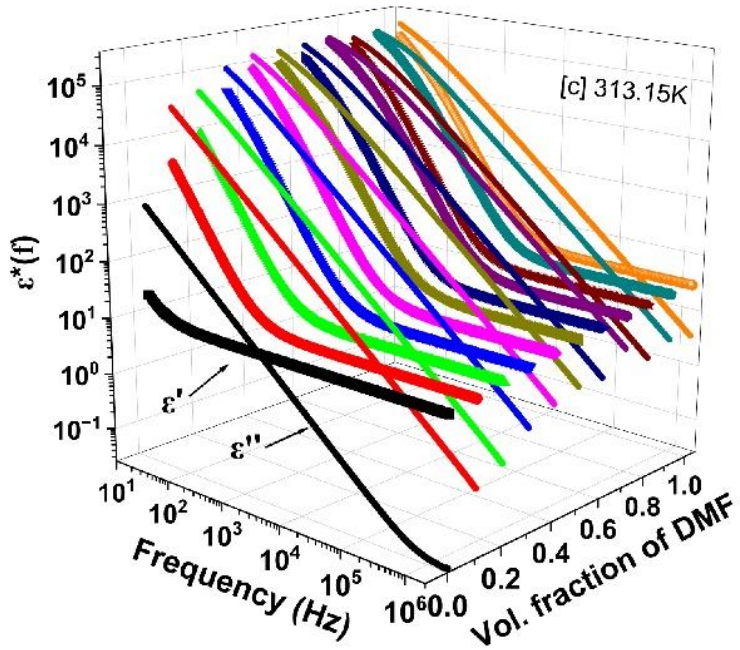

Fig. 5.1 (C) Variation of complex dielectric function ε*(f) against volume fraction of DMF in binary mixtures of all concentration range X_A = 0.0 to X_A= 1.0 at 313.15 K.

It is observed that the value of the real part of permittivity (ε′(f)) decreases as the temperature of the binary mixture increases. The low-frequency behavior of this liquid system indicates that pure DMF, pure n-Octanol, and their binary mixtures all include some amount of ionic contamination [51-53]. Many researchers have noted the presence of volatile ionic impurities in polar liquids, even in their purest state [20-22]. They have also observed that these unidentified charges significantly contributed to the dielectric behaviors of these liquids in the low-frequency regions and that the concentration of ionic impurities is proportional to the static permittivity of the polar liquids [23]. In investigations involving pure n-Octanol, pure N, N-Dimethylformamide (DMF), and their binary mixtures, the presence of ionic impurities has been detected, influencing the low-frequency behavior of the liquid system. The phenomenon of electrode polarization (EP) arises as ions migrate toward the electrode/sample interface under an electric field. This leads to the formation of double layers at the interface, introducing significant capacitances in series with the conducting bulk of the sample, characterized by high dielectric values in the lower frequency range [21,22]. Electric double layers (EDL capacitances) emerge at the interface between dielectric material and metallic electrode surfaces, attributed to the generation of ions and free charges across a considerable distance. Understanding these electric double layers is pivotal for

unraveling the complexities of the interplay between dielectric materials and metallic electrodes in this specific experimental setup [24-26]. The static dielectric permittivity (ε_0) values (10.07 (n-Octanol) and 37.92 (DMF)) of these n-Octanol DMF binary mixture at 293.15 K are considered equal to their ε' values at 2 MHz because these ε' values are independent of ionic contaminants. The (ε_0) values of n-Octanol-DMF mixtures at 303.15 K and 313.15 K are determined by capacitance measurements at 2 MHz only and these values are also given in table 5.1 along with the (ε_0) values at different temperatures. The imaginary $\varepsilon''(f)$ spectra of n-Octanol, DMF and their binary mixture decrease linearly with the increase of frequency up to 10^5 Hz and have slope equal to -1.00 ($\pm$ 0.02) is observed log -log scale at the different temperatures as shown in Figure 1, which confirms the ohmic type ionic conduction mechanism in these dipolar liquid mixtures. This behaviour was observed by many researchers for dipolar liquids and for binary mixtures [22,27-29]. The value of the imaginary part of the spectra decreases for all the concentration range as the temperature of the mixture increases.

In experimentally measured complex permittivity $\varepsilon^*(f)$ data in the frequency span 20 Hz to 2 MHz, electrode polarization effect is observed in the study of binary liquid mixtures. The Havriliak-Negami (HN) equation using Cole -Cole model, a concise dielectric relaxation model that accommodates asymmetric and broadened relaxation behavior [30,31] was used to fit the experimental data of complex permittivity spectra which is equation (4.1) (chapter 4). The experimental data of complex permittivity spectra was fitted to the equation (5) using a complex nonlinear least square (CNLS) [32] fitting method. $\Delta\varepsilon_{EP}$, ε_0 and τ_{EP} were used as fitting parameters are tabulated in table 5.2. Figure 5.2 (A) (B) and (C) shows the graph of experimental and fitted data to the Cole-Cole model of complex permittivity spectra for the concentration ranges (A) $X_A = 0.000$, (B) $X_A = 0.5$, and (C) $X_A = 1.0$ at different temperatures. The Cole-Cole model provides a good match to the results of experiments at different temperatures. Different fitting parameters are tabulated in Table 5.2. Values of the electrode polarization relaxation time increases as the temperature increases for pure Octanol and DMF. Electrode polarization relaxation time (τ_{EP}) is the amount of time required to cease the transfer of charges between the sample and electrode, and this results to the formation of an electrode double layer [33]. Electrode polarization relaxation time (τ_{EP}) of pure liquid (n- Octanol) mixtures is 682.69 ms and drops to 43.28 ms for

concentration X_A = 0.1 volume fraction of DMF in this mixture at 293.15 K temperature. It can be observed from Table 5.2 that value of static dielectric constant decreases with increase in temperatures. Values of the $\Delta\varepsilon_{EP}$ and electrode polarization relaxation time changes anomalously as the concentration of the mixture increases. Static dielectric constant value decreases as the concentration of the mixture increases for all the different temperatures.

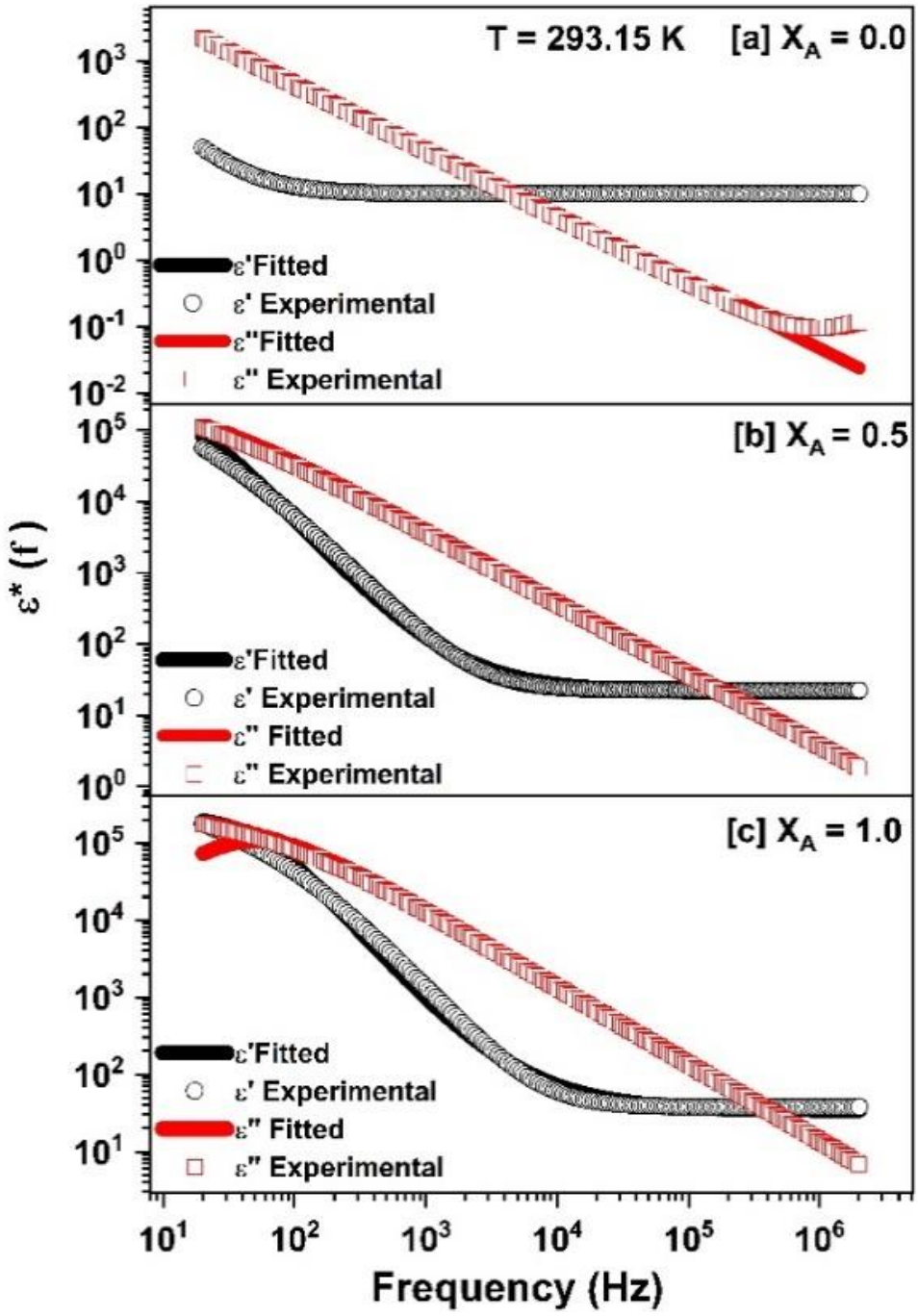

Fig.5.2 (A) Complex dielectric function (ε*(f)) fitted to Cole-Cole model by CNLS method for different concentration X_A = 0.0. X_A = 0.5 and X_A = 1.0 at 293.15 K.

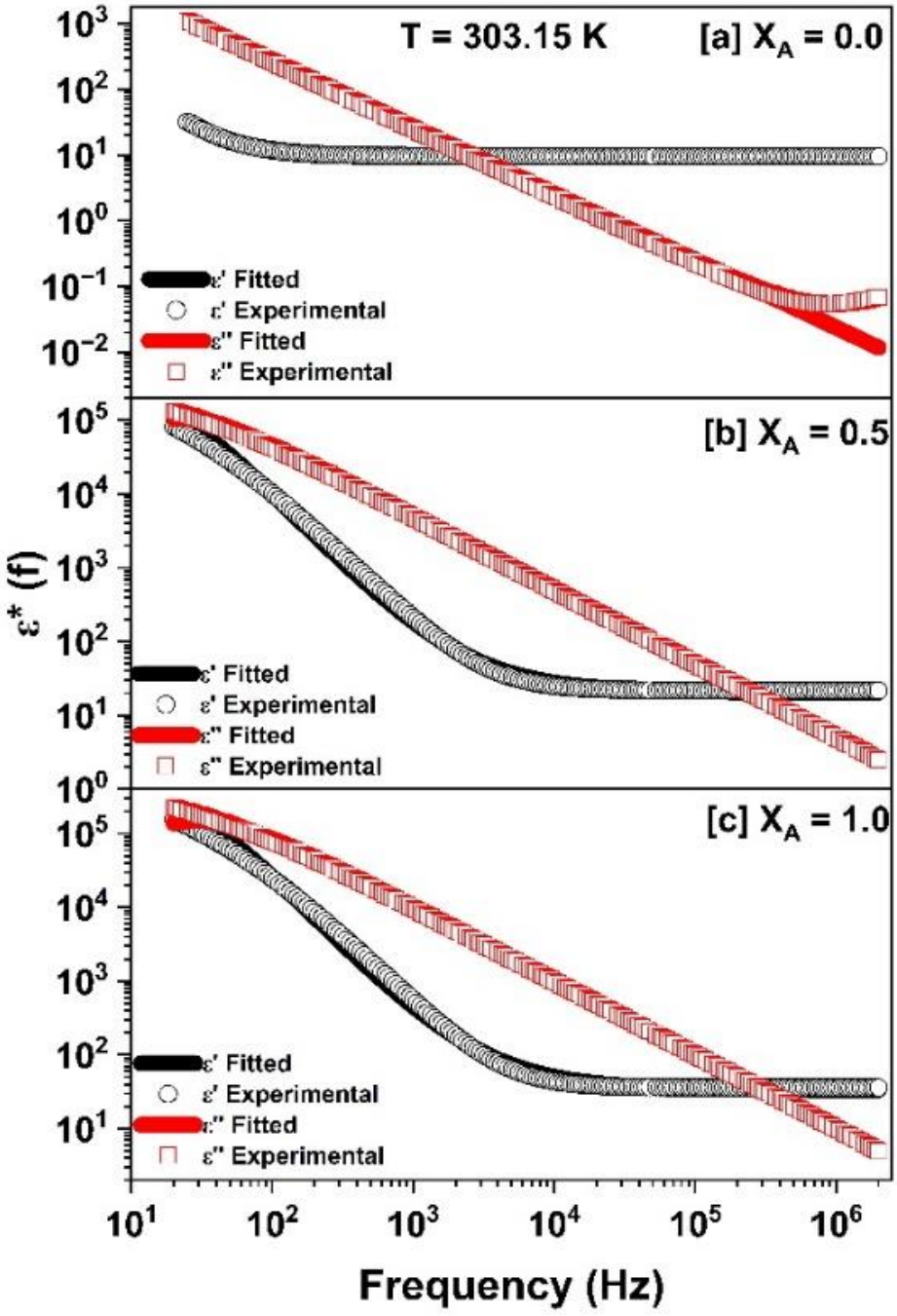

Fig.5.2 (B) Complex dielectric function (ε*(f)) fitted to Cole-Cole model by CNLS method for different concentration $X_A = 0.0$. $X_A = 0.5$ and $X_A = 1.0$ at 303.15 K.

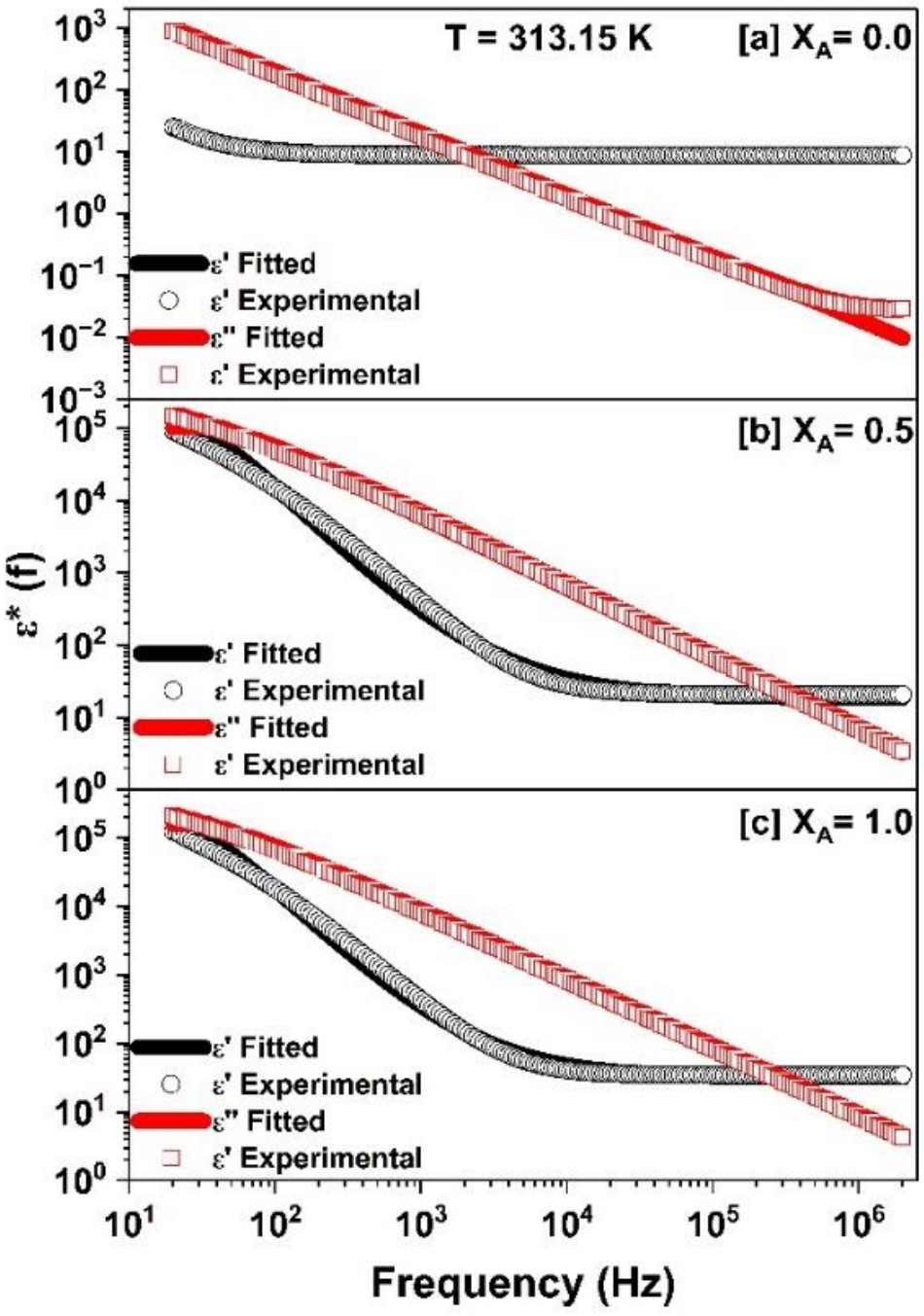

Fig.5.2 (C) Complex dielectric function (ε*(f)) fitted to Cole-Cole model by CNLS method for different concentration X_A = 0.0. X_A = 0.5 and X_A = 1.0 at 313.15 K.

Table 5.2 Fitted values of the parameters ε_0, $\Delta\varepsilon_{EP}$, τ_{EP} and α of the Cole - Cole model for binary mixtures of Octanol and DMF at different temperatures.

X_A	ε_0	$\Delta\varepsilon_{EP}$	τ (ms)	α
T= 293.15 K				
0.0	9.98	1.92 E+05	682.69	0.99
0.1	11.17	2.38E+05	43.288	0.99
0.2	13.54	2.00E+05	35.20	0.99
0.3	16.01	2.19E+05	22.23	0.99
0.4	19.13	2.55E+05	11.75	0.97
0.5	21.25	2.19E+05	10.45	0.99
0.6	24.36	1.88E+05	5.68	0.98
0.7	26.62	2.05E+05	3.98	0.98
0.8	29.31	1.94E+05	3.94	0.98
0.9	33.19	2.67E+05	3.21	0.98
1.0	34.24	2.21E+05	3.00	0.98
T= 303.15 K				
0.0	9.48	1.01E+05	748.70	0.99
0.1	10.73	2.77E+05	68.66	0.99
0.2	13.04	2.31E+05	35.32	0.99
0.3	15.30	2.35E+05	17.25	0.99
0.4	17.84	2.33E+05	11.12	0.99
0.5	20.43	2.14E+05	7.51	0.99
0.6	23.38	2.22E+05	8.55	0.99
0.7	25.85	2.18E+05	5.91	0.99
0.8	27.99	1.39E+05	4.68	0.98
0.9	30.71	2.71E+05	1.79	0.98
1.0	33.44	3.02E+05	5.37	0.99
T= 313.15 K				
0.0	8.70	1.20E+05	1070.20	0.99
0.1	10.23	3.11E+05	68.26	0.99
0.2	12.46	2.70E+05	36.63	0.99

0.3	14.66	2.70E+05	14.93	0.99
0.4	17.77	3.08E+05	10.60	0.98
0.5	18.84	2.18E+05	6.12	0.98
0.6	23.08	3.16E+05	9.05	0.98
0.7	23.69	2.31E+05	3.18	0.99
0.8	27.43	2.24E+05	5.59	0.98
0.9	29.94	2.30E+05	3.91	0.98
1.0	31.57	3.25E+05	7.00	0.98

Figure 5.3. (A), (B) and (C) shows the frequency and concentration dependent loss tangent (tan δ) graph of the binary mixtures at different temperatures. It can be observed that the maxima peak for the mixtures is shifting towards lower frequency region as the concentration of the n-Octanol increases in the mixture. The systematic variation in the maxima peak of the loss tangent (tan δ) for all the temperature range is observed. As the temperature of the mixtures increases, the maxima peak shifts towards the lower frequency side in the frequency spam.

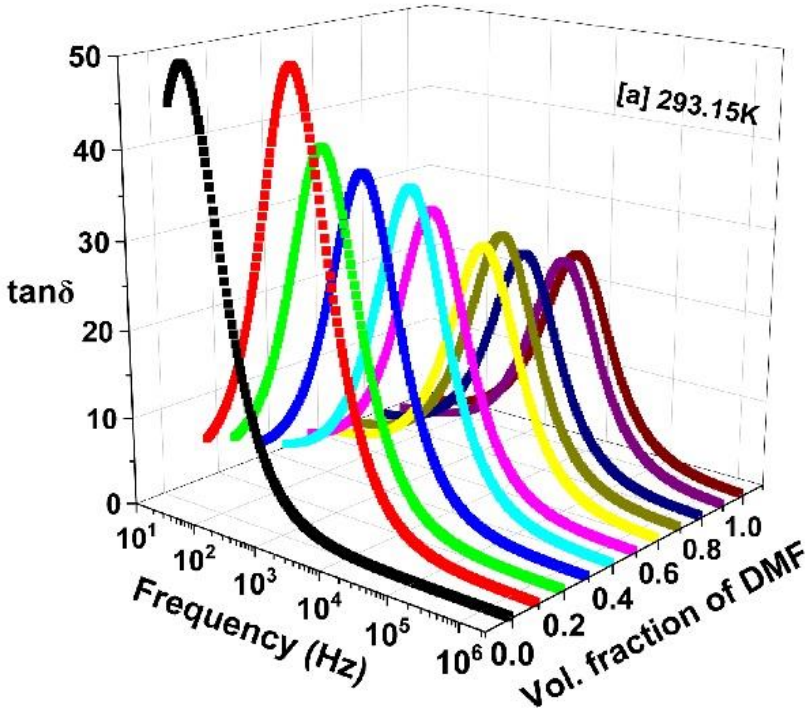

Fig.5.3 (A) Variation of the tan δ for concentration range X_A = 0.0 to X_A= 1.0 at 293.15 K.

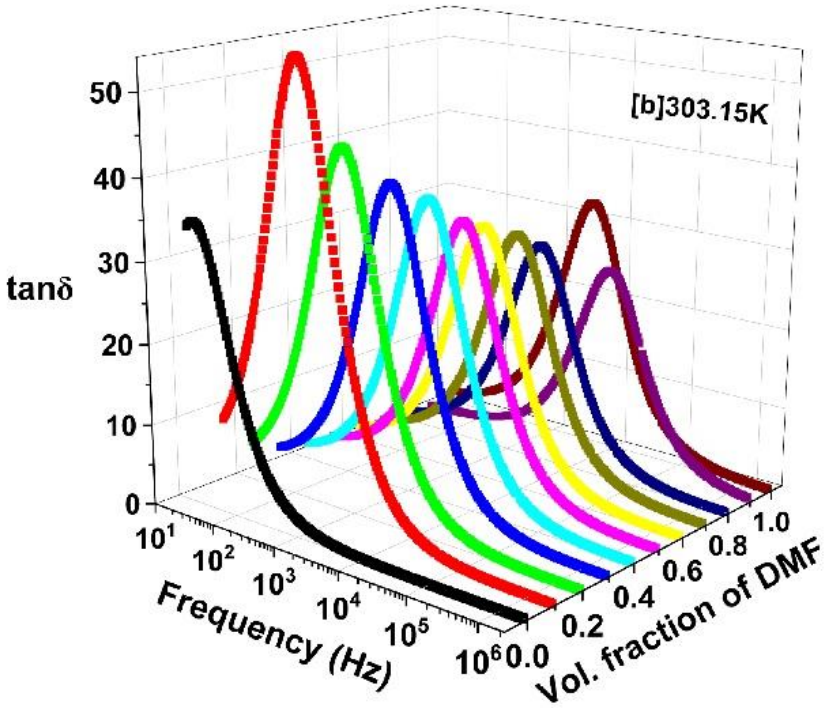

Fig.5.3 (B) Variation of the tan δ for concentration range X_A = 0.0 to X_A= 1.0 at 303.15 K.

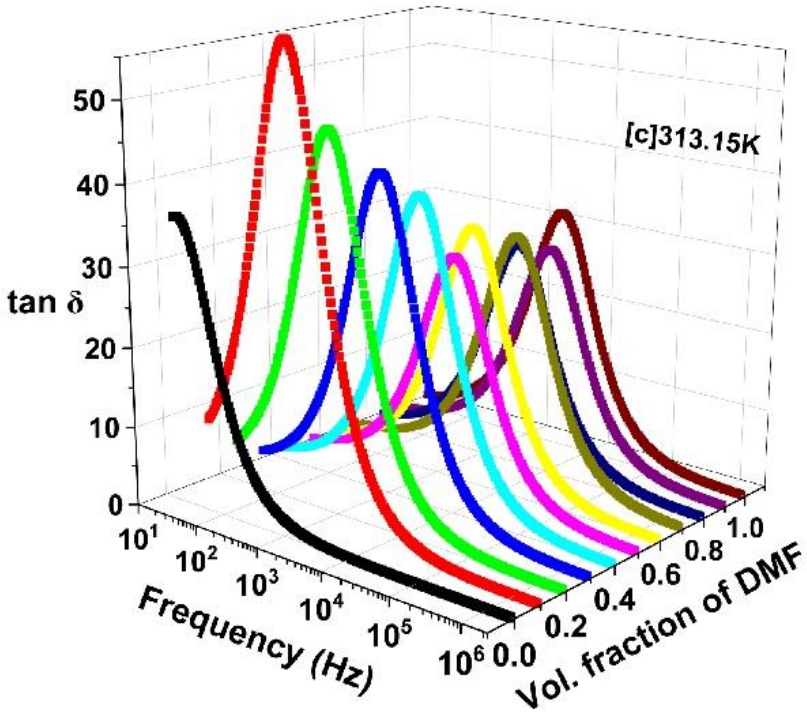

Fig.5.3 (C) Variation of the tan δ for concentration range X_A = 0.0 to X_A= 1.0 at 313.15 K.

The value of the dielectric constant for pure n-Octanol is low in comparison of DMF but the behavior of the maxima peak is in the opposite manner, means maxima peak for

n-Octanol is high in comparison of other material. The relaxation frequency f_{EP}' that separates the bulk phenomenon from the conductivity phenomenon at the dielectric/electrode interface is equivalent to the peak value of the observed loss tangent (tan δ) value [34]. The relaxation frequency (τ'_{EP}) used to evaluate relaxation time, which is given by relation $\tau'_{EP} = \left(\frac{1}{2\pi f_{EP'}}\right)$ [34,35]. The τ'_{EP} values for different temperatures and different concentration range X_A=0.0 to X_A=1.0 is tabulated in Table 5.3. The observed table 5.3 value of the relaxation time for the pure octanol is at 4477.24 ms at 293.15 K temperature and increases till 7516.40 ms as the temperature increases up to 313.15 K temperature. The similar type of behavior is observed for DMF. It shows the amanous behavior for the binary mixtures of n-Octanol+DMF. Figure 5.4 (A), (B) and (C) shows the change of the normalized loss tangent ($\frac{\tan\delta}{\tan\delta_{max}}$) as a function of the normalized frequency ($\frac{f}{f_{max}}$) for concentration range 0.000≤ X_A ≤1.00 [1]. It is seen from the graph that the data points exhibit perfect overlapping for all the concentration ranges at different temperatures. It represents that the EDL phenomena in mixtures are concentration-independent and follows the same dynamical mechanism [24].

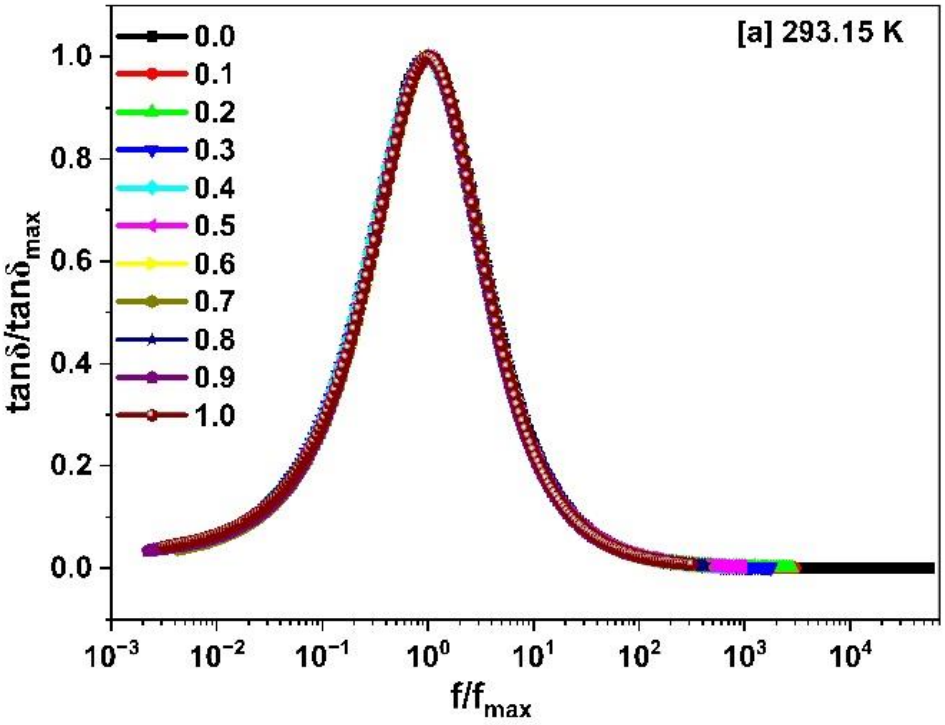

Fig. 5.4 (A) Normalized loss tangent (tan δ/tan δ max) as a function of normalized frequency (f/f_{max}) for all the concentration range at 293.15 K.

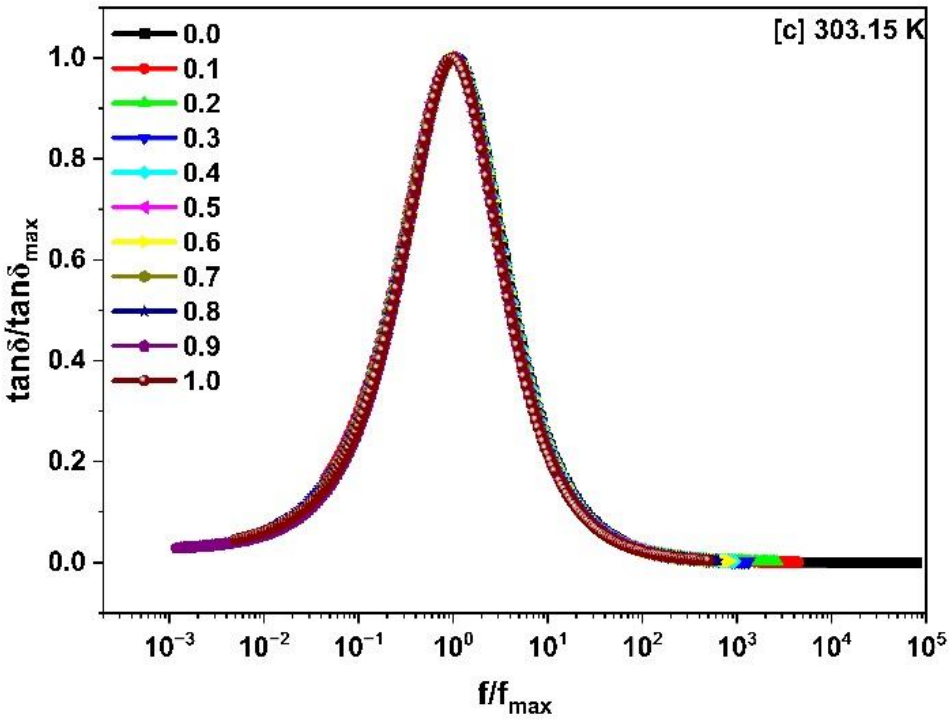

Fig. 5.4 (B) Normalized loss tangent (tan δ/tan δ max) as a function of normalized frequency (f/f_{max}) for all the concentration range at 303.15 K.

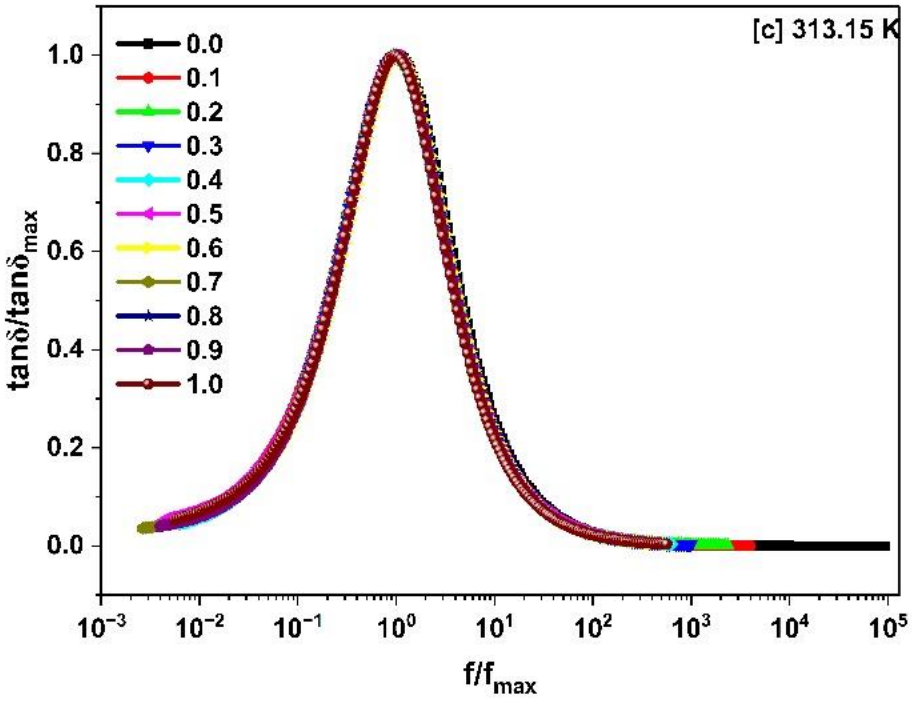

Fig. 5.4 (C) Normalized loss tangent (tan δ/tan δ max) as a function of normalized frequency (f/f_{max}) for all the concentration range at 313.15 K.

5.3.1.2 Electrical Modulus Spectra

The electric modulus spectrum is useful for studying the ionic conductivity relaxation process occurring in polar liquids. The space charge effect in dielectric spectra is overcome by electric modulus spectra [35]. Figure 5. 5 (A), (B) and (C) shows the frequency dependent real (M′(f)) and imaginary(M′′(f)) parts of the complex modulus spectra (M*(f)) for all concentration at different temperatures respectively. From the figure, it can be seen that the real part of (M′(f)) values lower concentration of pure n-Octanol in the lower frequency span (≤ 10^3 Hz) are relatively very high and systematically decrease at different temperatures. In mid-frequency span for lower concentration of n-Octanol, the value of real part (M′(f)) decrease with increase in frequency span, approaching a constant level in the MHz range of frequency span at different temperatures similarly effect. The M′(f) values for concentration range X_A= 0.9 and X_A= 1.0 remain constant through the entire frequency span. The M"(f) spectrum exhibits dispersion in the frequency region between f_{EP}′ and f_σ, which corresponds to the tanδ and M" peaks, respectively. All binary mixtures exhibit the peak in the imaginary part of the electric modulus at all temperatures.

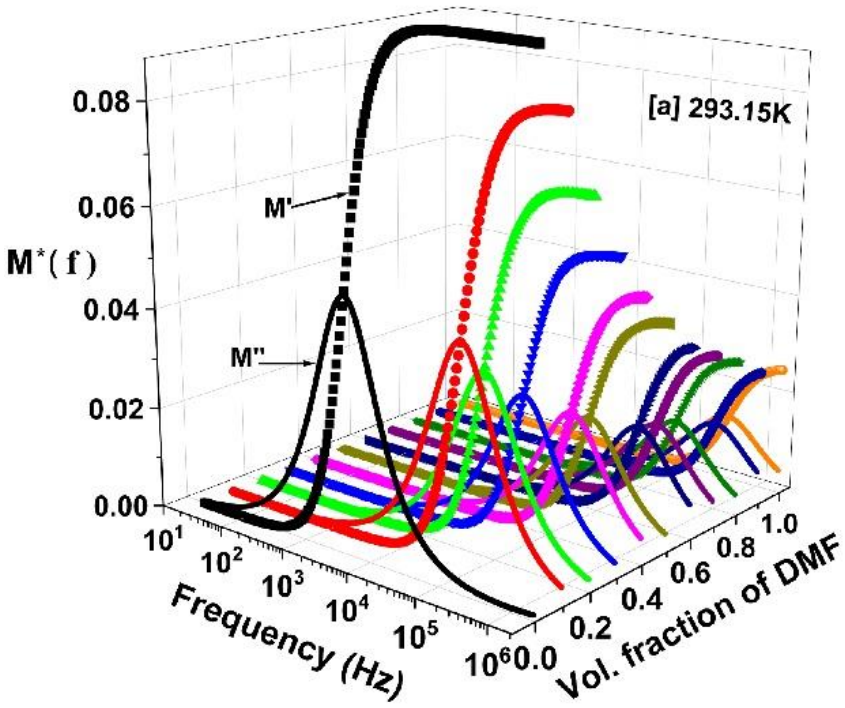

Fig. 5.5 (A) Variation of electric modulus function M*(f) for the variation concentration range X_A = 0.0 to X_A= 1.0 at 293.15 K.

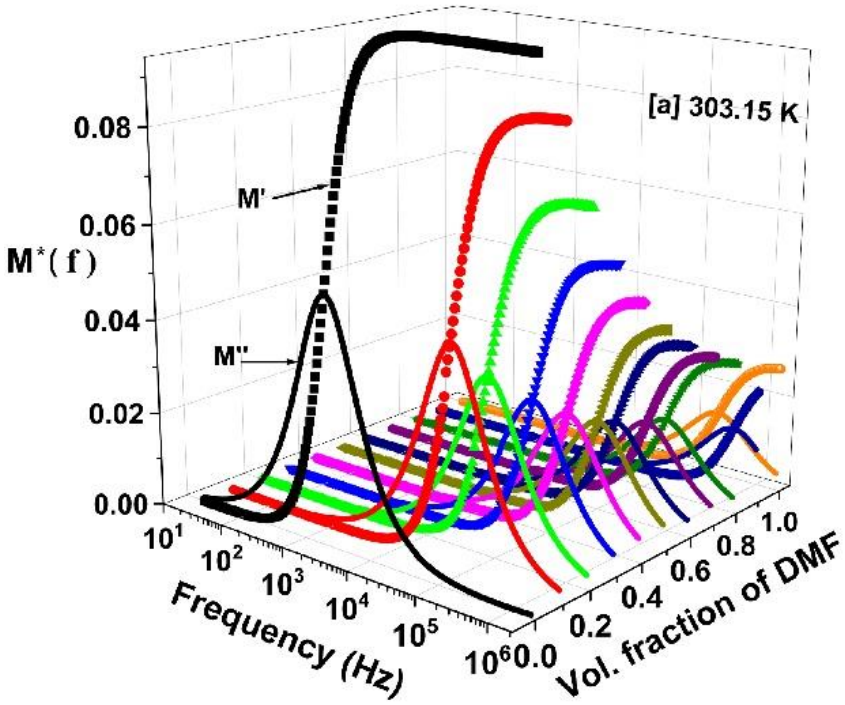

Fig. 5.5 (B) Variation of electric modulus function M*(f) for the variation concentration range X_A = 0.0 to X_A= 1.0 at 303.15 K.

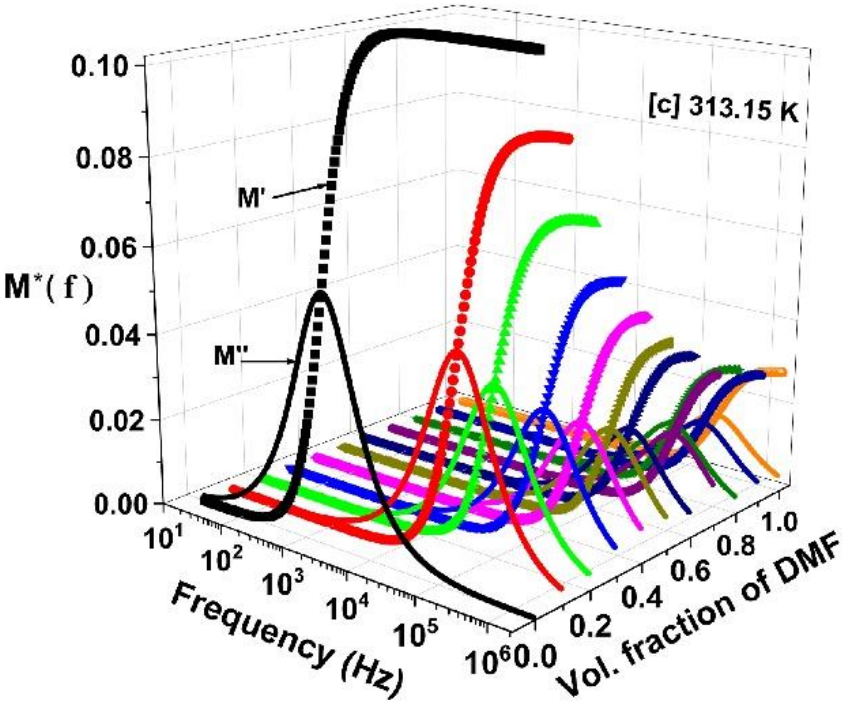

Fig. 5.5 (C) Variation of electric modulus function M*(f) for the variation concentration range X_A = 0.0 to X_A= 1.0 at 313.15 K.

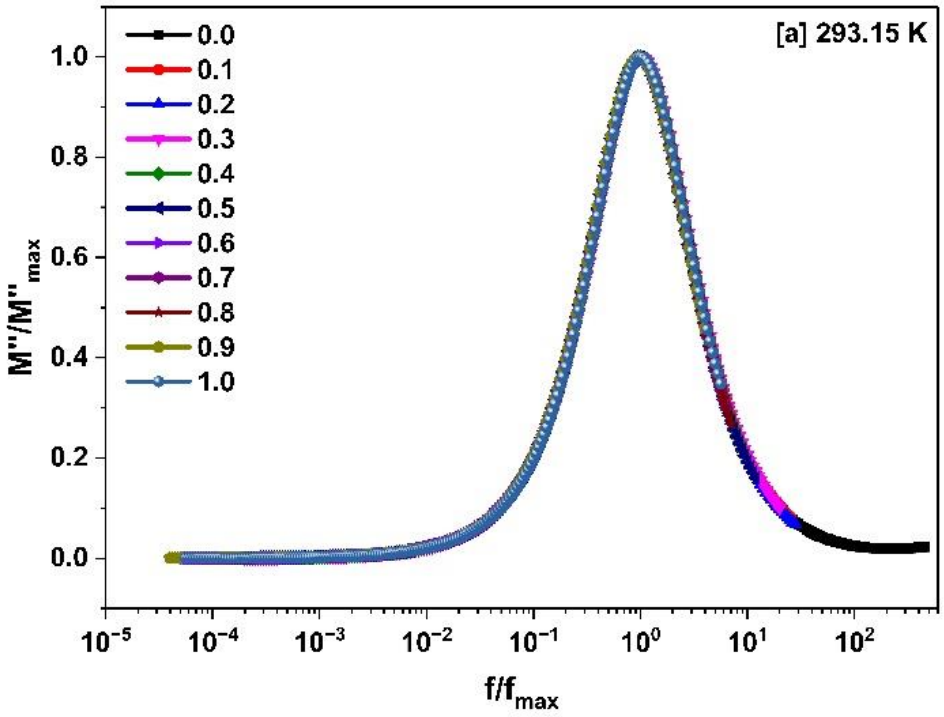

Fig. 5.6 (A) Normalized imaginary part of the electric modulus for all concentration range X_A = 0.0 to X_A= 1.0 at 293.15 K.

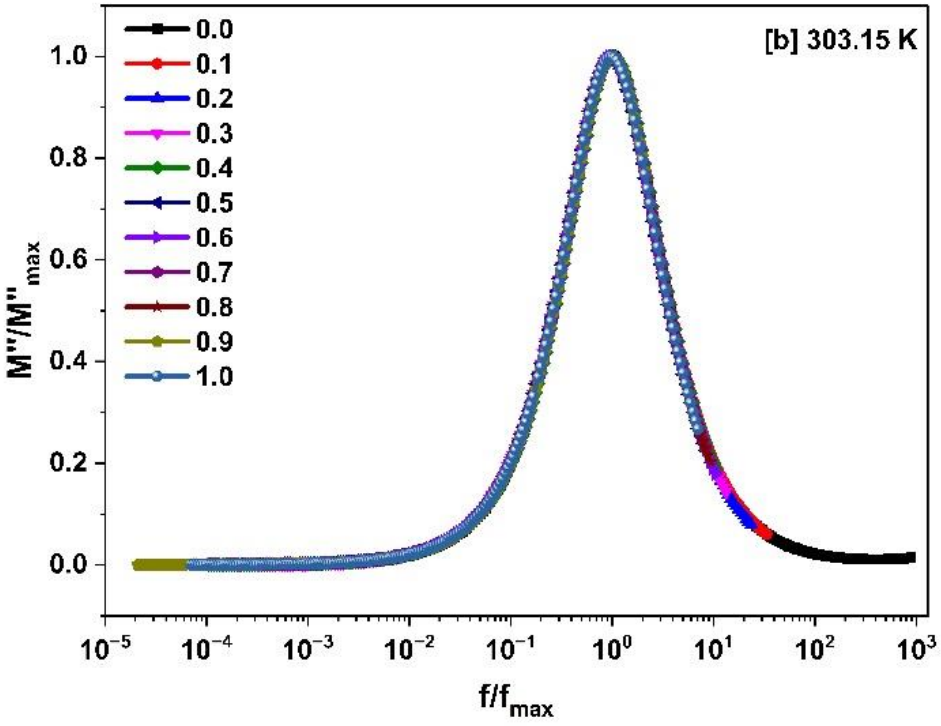

Fig. 5.6 (B) Normalized imaginary part of the electric modulus for all concentration range X_A = 0.0 to X_A= 1.0 at 303.15 K.

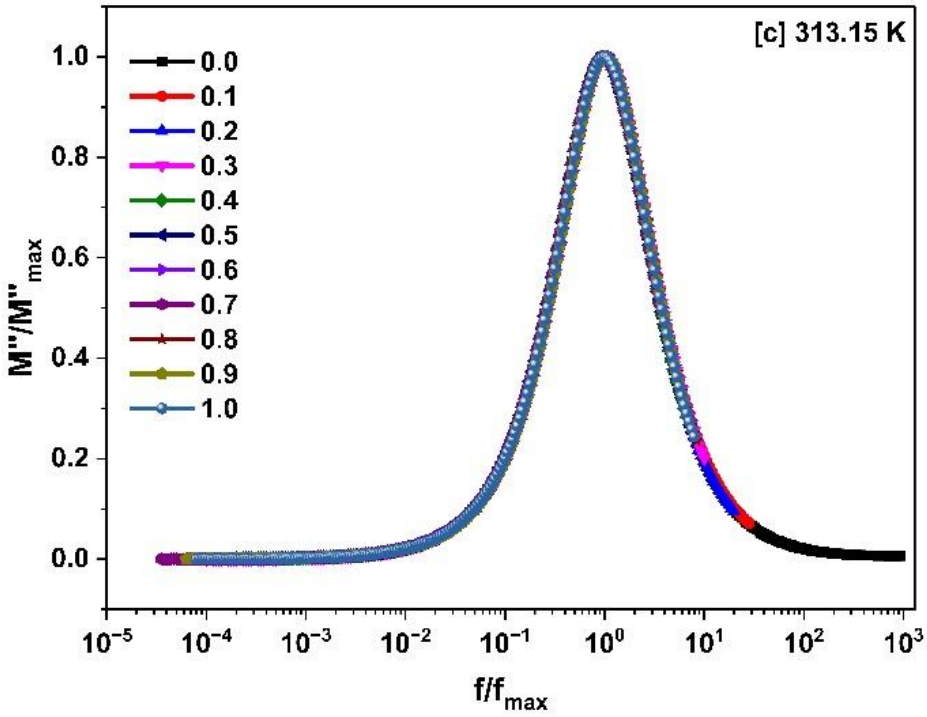

Fig. 5.6 (C) Normalized imaginary part of the electric modulus for all concentration range X_A = 0.0 to X_A= 1.0 at 313.15 K.

The observed imaginary part M"(f) peak is in the lower frequency region for the lower concentration of n-Octanol and as the volume fraction of DMF increases the peak is shifted towards the higher frequency span. The same behaviour is observed at different temperatures. The frequency f_σ corresponding to the maximum value of M" is related to the relaxation time of ionic conductivity, $\tau_\sigma = \frac{1}{2\pi f_\sigma}$ [36,37]. Variation in the conductivity relaxation time (τ_σ) with the change in the volume fraction of DMF at different temperatures is tabulated in Table 5.3. The value of the ionic relaxation time increases for the pure n-Octanol and DMF as the temperature increases. Ionic relaxation time shows amanous behavior for the mixtures. The variation of the normalized loss part of the electric modulus $(\frac{M''}{M''_{max}})$ as a function of the normalized frequency $(\frac{f}{f_{max}})$ at different temperatures is shown in Figure 5.6 (A), (B) and (C). The experimental data points for every concentration and all temperatures on the graph overlap on a single curve, indicating that the M" spectra is of the Debye-type [24]. Figure 5.7 shows the electric modulus spectra (M*(f)) for the (Imaginary part (M′′(f)) versus real part (M′(f))) for the different concentration range X_A=0.0 to X_A=1.0 at different temperatures. Debye- Semicircle is observed in different concentrations at different

temperatures. Similar type of behaviour is observed in different modulus formalism by many researchers [24,35,38].

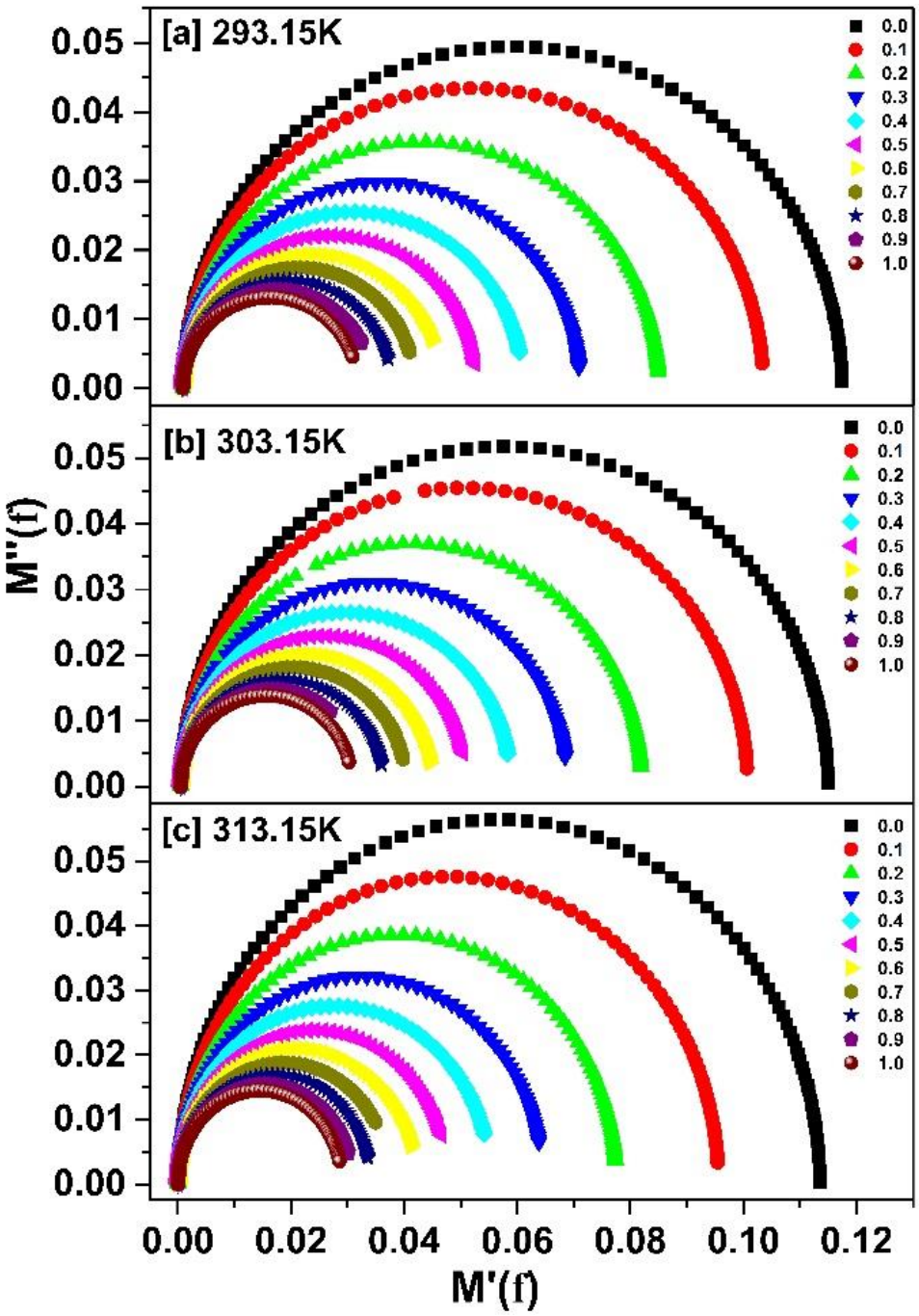

Fig. 5.7 The electric modulus spectra of the binary mixtures of n-Octanol and N, N-Dimethylformamide in complex plane at [a] 293.15 K, [b] 303.15 K, [c] 313.15 K temperatures.

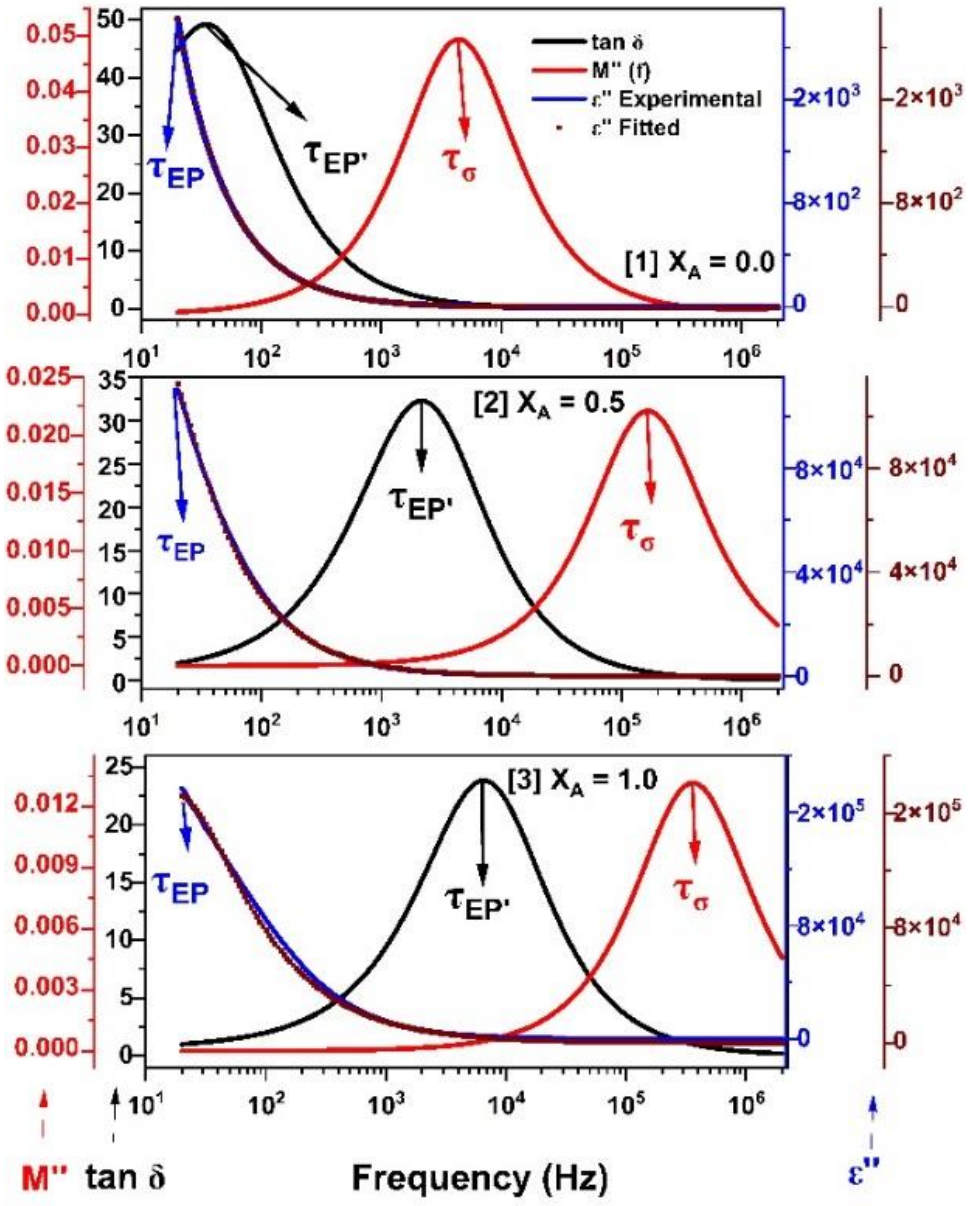

Fig. 5.8 (A) Relation between τ_{EP}, $\tau_{EP'}$ and τ_{σ} for concentration $X_A = 0.0$, $X_A = 0.5$. and $X_A = 1.0$ at 293.15 K.

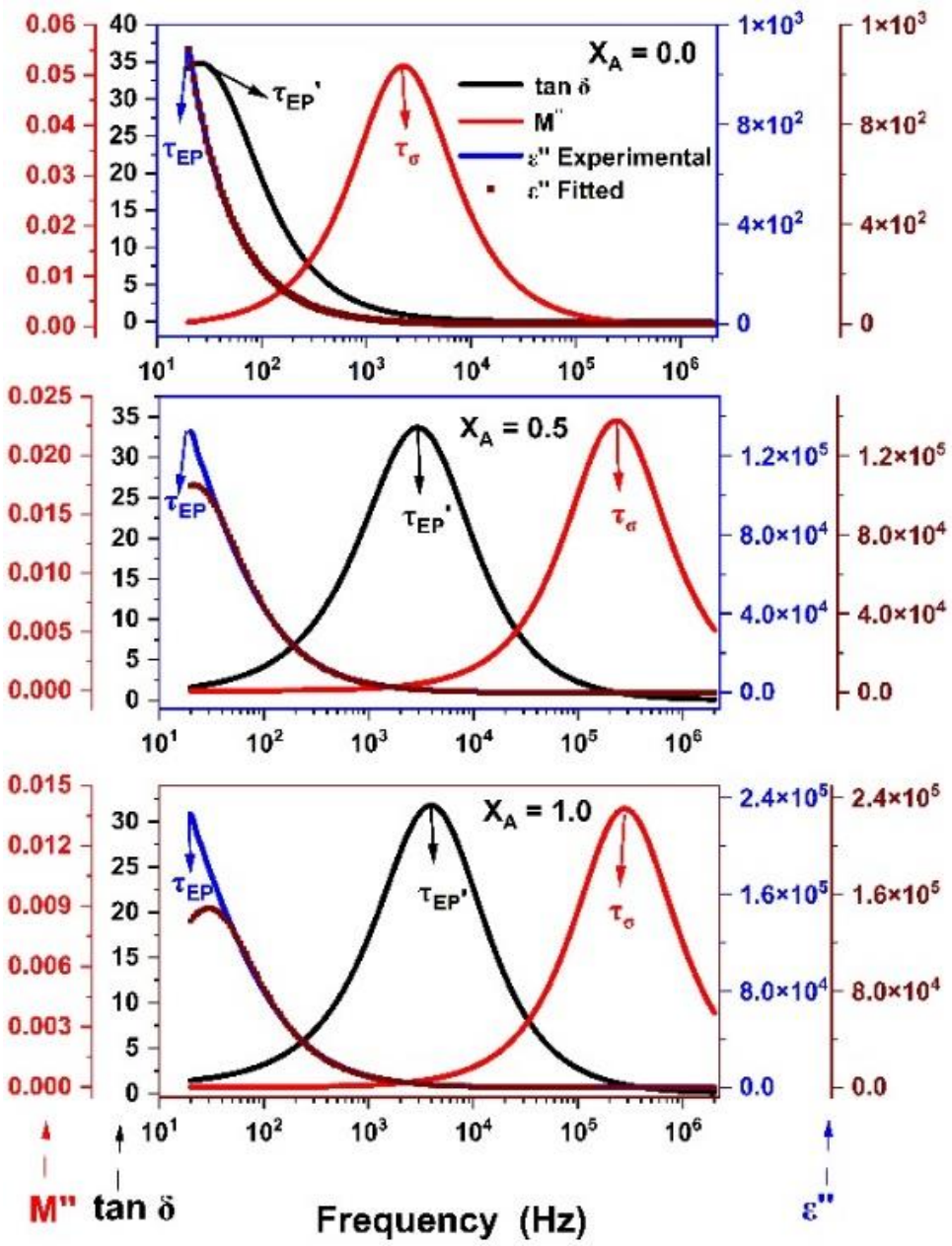

Fig. 5.8 (B) Relation between τ_{EP}, $\tau_{EP'}$ and τ_{σ} for concentration $X_A = 0.0$, $X_A = 0.5$. and $X_A = 1.0$ at 303.15 K.

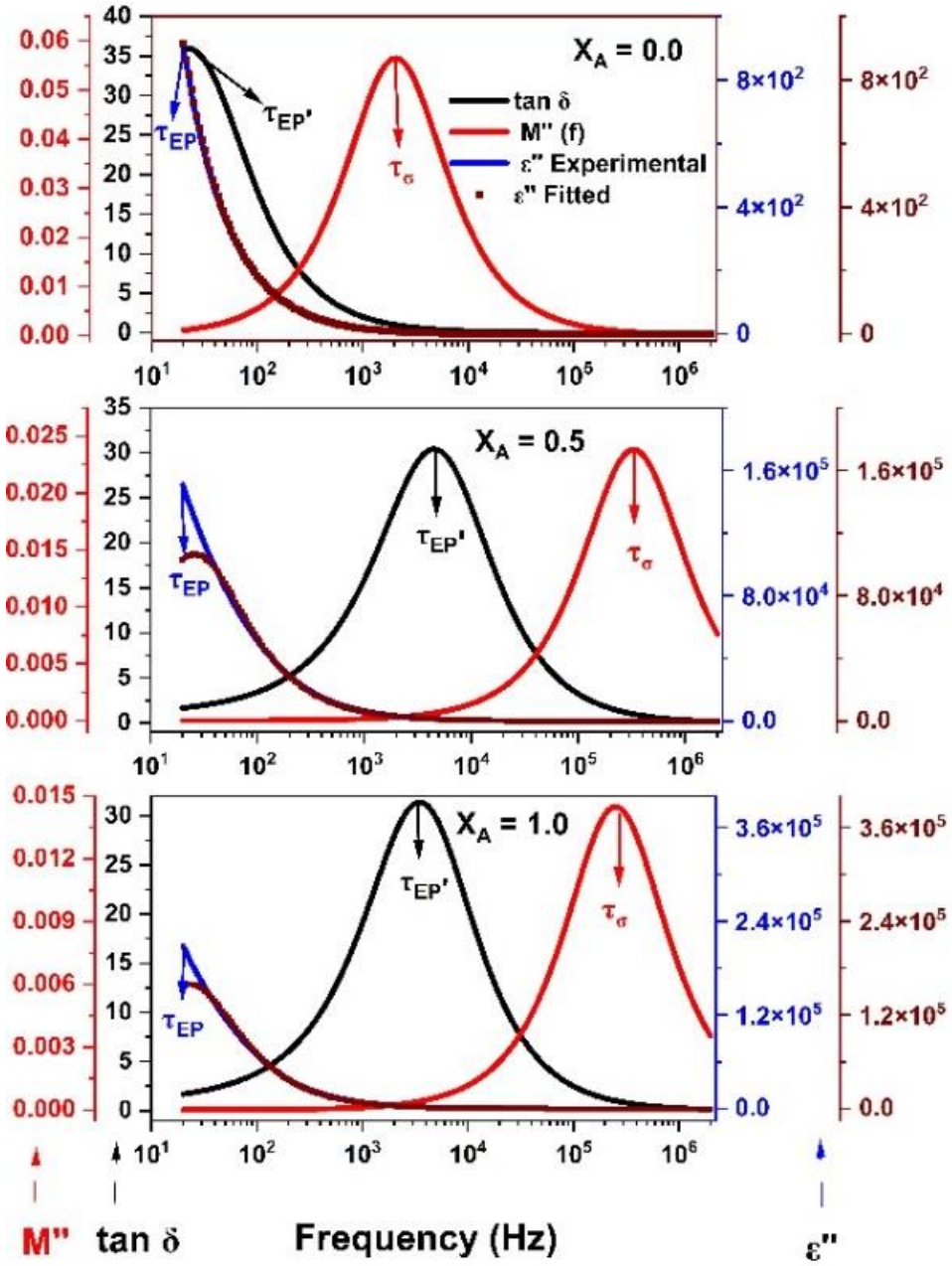

Fig. 5.8 (C) Relation between τ_{EP}, $\tau_{EP'}$ and τ_{σ} for concentration $X_A = 0.0$, $X_A = 0.5$. and $X_A = 1.0$ at 313.15 K.s

Figure 8 (A), (B) and (C) shows the different relaxation phenomena on a single scale. The variation of τ_{EP}, $\tau_{EP'}$ and τ_{σ} for concentration $X_A = 0.0$, $X_A = 0.5$. and $X_A = 1.0$ for the different temperature ranges are shown in Figure 8. The relaxation time (τ_{EP}) is obtained from imaginary part of permittivity spectra (ε''), τ'_{EP} is derived from loss tangent ($\tan\delta$) and τ_{σ} is derived from Imaginary part of modulus (M'') spectra. It can be seen from the graph that for all the concentration ranges the peak is shifting towards

the higher frequency region as the concentration of the mixture increases. The reverse trend is observed with the temperature as the concentration increases of the mixtures, it shifts towards the lower frequency region. Three different relaxation time in the studied system are correlated by relation $\tau'_{EP} = (\tau_{EP} \times \tau_{\sigma})^{\frac{1}{2}}$ [29,39]. Many researchers observed the similar type of relation in the binary mixture [34,35,39,40].

5.3.1.3 Electric Conductivity Spectra

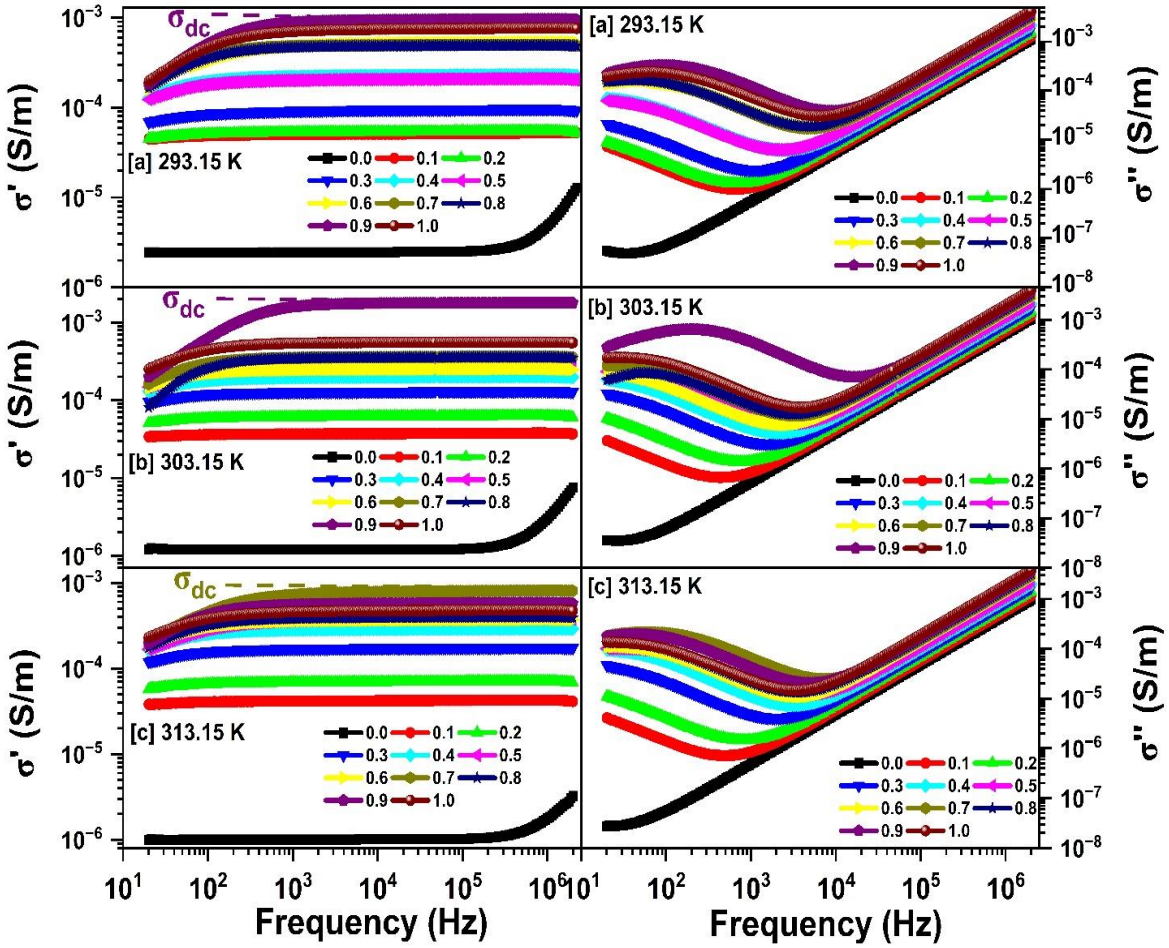

Fig. 5. 9 (A) Real (σ′) and (B) imaginary (σ′′) parts of binary mixtures of all concentration range of $X_A = 0.0$ to $X_A = 1.0$ at [a] 293.15 K, [b] 303.15 K, [c] 313.15 K temperatures.

The real part of complex ac conductivity σ′(ω) are determined using the equation (3.9). Figure 5.9 (A), (B) and (C) shows the real part conductivity (σ′) against the frequency of concentration for the binary mixture of all concentration range of $X_A = 0.0$ to $X_A = 1.0$ at different temperature ranges [293.15 K, 303.15 K and 313.15K]. Values of the σ'(f) spectra increases up to the frequency range 10^4 Hz for the higher concentration of the DMF then it remains the constant in higher frequency range. While for the higher concentration of the DMF, it shows a slight increasing trend then it remains constant.

σ'(f) values decrease as the temperature increase for the DMF and in the mixtures but it shows inverse trend for pure n-Octanol. In this Figure 5.9, σ'(f) spectra have a frequency-independent plateau area that extrapolates to the σ'(f) axis, and the intercepted value of' σ′ is taken to be considered as the dc conductivity (σ_{dc}) [34].

The σ_{dc} values for the n-Octanol + DMF systems is determined from the spectra's low frequency steady-state behavior (shown by solid horizontal lines). σ_{dc} values observed at all concentration and all temperature are tabulated in Table 5.3. σ_{dc} values for X_A = 0.0 is 2.47 μS/m and for X_A = 1.0 is 74.27 μS/m at 293.15 K. It shows that values of the dc conductivity increase as the concentration of the mixture increases for the higher concentration of DMF. Values of the DC conductivity increases with the increase in temperature for all the concentration ranges. Figure 5.9 (a), (b) and (c) shows the imaginary part of σ′′(f) versus frequency (log-lag scale) for volume fraction of DMF in n-Octanol + DMF system at different temperatures. Minima peak is observed in the σ′′(f) spectra for all the concentration ranges in all the temperature ranges. The peak is shifting towards the lower frequency region as the concentration of DMF increases in the mixtures. Minima and maxima peaks are observed for the pure DMF and for the higher concentration of the DMF. Mimina and maxima peak is shifting from lower frequency to higher frequency side as the temperature of the mixture increases. It can be predicted that σ"(f) spectra can also be used to understand the dynamics of EDLs in dipolar liquids [34] because the frequency corresponding to the σ"(f) minimum is the same as the frequency of the tanδ peak in Figure 5.3.

Table 5.3 Variation of relaxation time (τ_{EP}'), ionic polarization relaxation time (τ_σ) and DC electrical conductivity (σ_{dc}) for different Volume fraction of DMF in n-Octanol+ DMF system at different temperatures.

X_A	τ_{EP}' (μS)	τ_σ (μS)	σ_{dc} (μ S)
T=293.15 K			
0.0	4477.24	35.56	2.49
0.1	237.69	2.00	51.52
0.2	224.39	2.24	53.33
0.3	141.58	1.59	95.92
0.4	63.24	0.75	228.01
0.5	75.16	0.95	207.65
0.6	28.25	0.42	522.28

0.7	33.57	0.50	502.32
0.8	33.57	0.56	490.22
0.9	17.82	0.32	952.87
1.0	25.18	0.45	744.79
T=303.15 K			
0.0	6324.27	70.96	1.25
0.1	355.64	2.67	37.38
0.2	211.84	1.89	61.71
0.3	106.17	1.06	129.74
0.4	75.16	0.84	203.13
0.5	53.21	0.67	279.97
0.6	66.99	0.84	253.65
0.7	47.43	0.67	362.55
0.8	50.24	0.75	357.59
0.9	9.46	0.17	1787.74
1.0	39.90	0.56	552.88
T=313.15 K			
0.0	7516.40	75.16	1.01
0.1	316.96	2.24	42.00
0.2	188.80	1.59	68.90
0.3	79.62	0.80	174.40
0.4	50.24	0.53	291.86
0.5	35.56	0.47	377.63
0.6	44.77	0.56	368.98
0.7	21.18	0.30	803.58
0.8	44.77	0.67	394.66
0.9	31.70	0.50	574.89
1.0	44.77	0.63	467.45

5.3.1.4 Complex Impedance Spectra

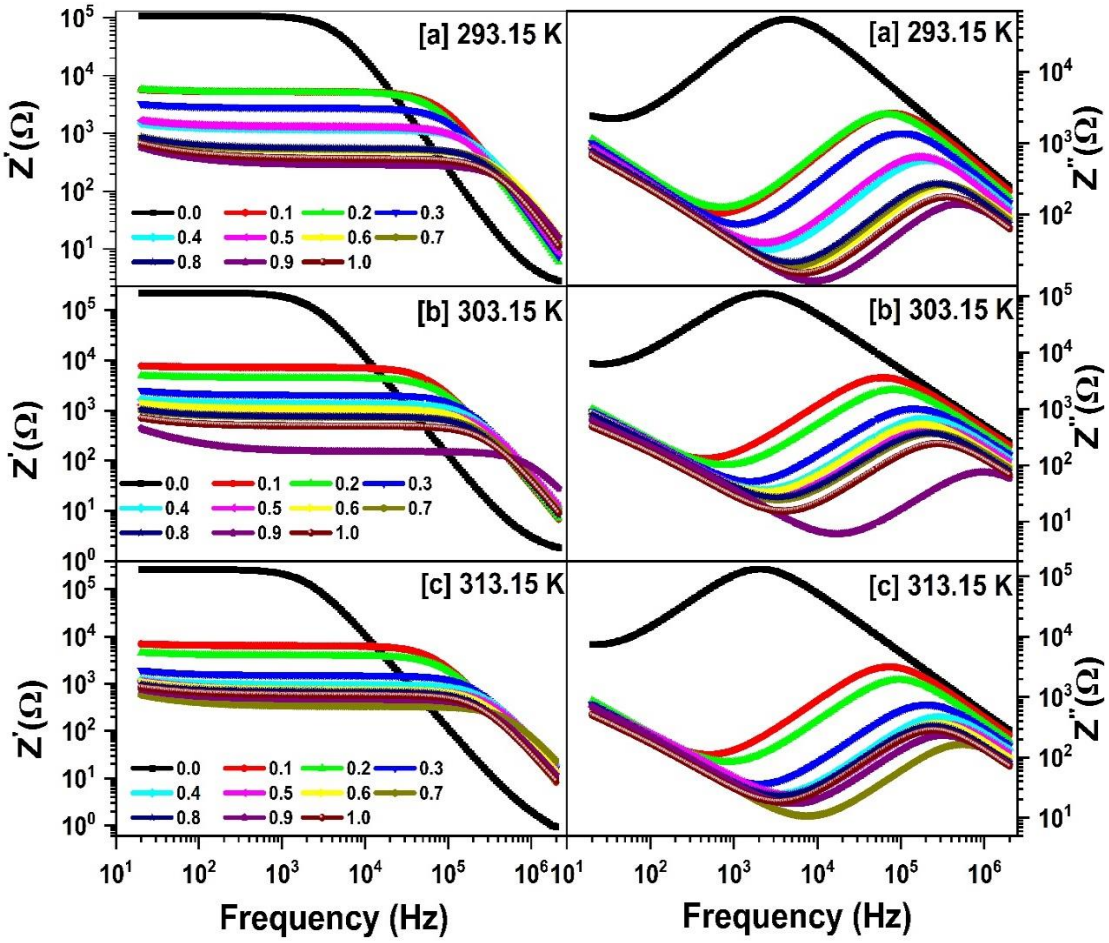

Fig. 5.10 (A) Real (Z′(f)) and (B) imaginary (Z" (f)) parts of complex impedance (Z^* (f)) for binary mixtures of all concentration range of X_A = 0.0 to X_A= 1.0 at [a] 293.15 K, [b] 303.15 K, [c] 313.15 K temperatures.

In the low-frequency region of dielectric spectroscopic spectra, most polar liquid materials exhibit both electric double-layer (EDL) and conductivity relaxation processes. These phenomena are identified by analyzing the imaginary component of the complex impedance spectra [26]. To investigate these processes, the complex impedance Z*(ω) of the binary mixtures was determined using the experimentally measured values of parallel capacitance (C_P) and parallel resistance (R_P), as described by Equation (3.10). Figure 5.10 (A) and (B) represent the spectra of Z′(f) and Z″(f) for the different concentration and temperature ranges. Notably, the real part of impedance Z′(f) exhibits a gradual decrease with increasing frequency in the low and intermediate frequency ranges, while it sharply decreases in the high-frequency region. Concurrently, the Z″(f) spectra display a significant decrease in the low-frequency range, reaching a minimum in the mid-frequency region. Beyond these frequencies,

Z″(f) values increase, culminating in a peak in the high-frequency region. The observed shift of the relaxation peak in Z″(f) towards higher frequencies, coupled with a decrease in magnitude at elevated temperatures, suggests enhanced charge mobility in thermally activated dielectric systems [26]. Moreover, at a fixed frequency, both Z′(f) and Z″(f) values decrease with rising temperature, indicating the semiconducting behavior of the n-Octanol + DMF binary liquid mixtures.

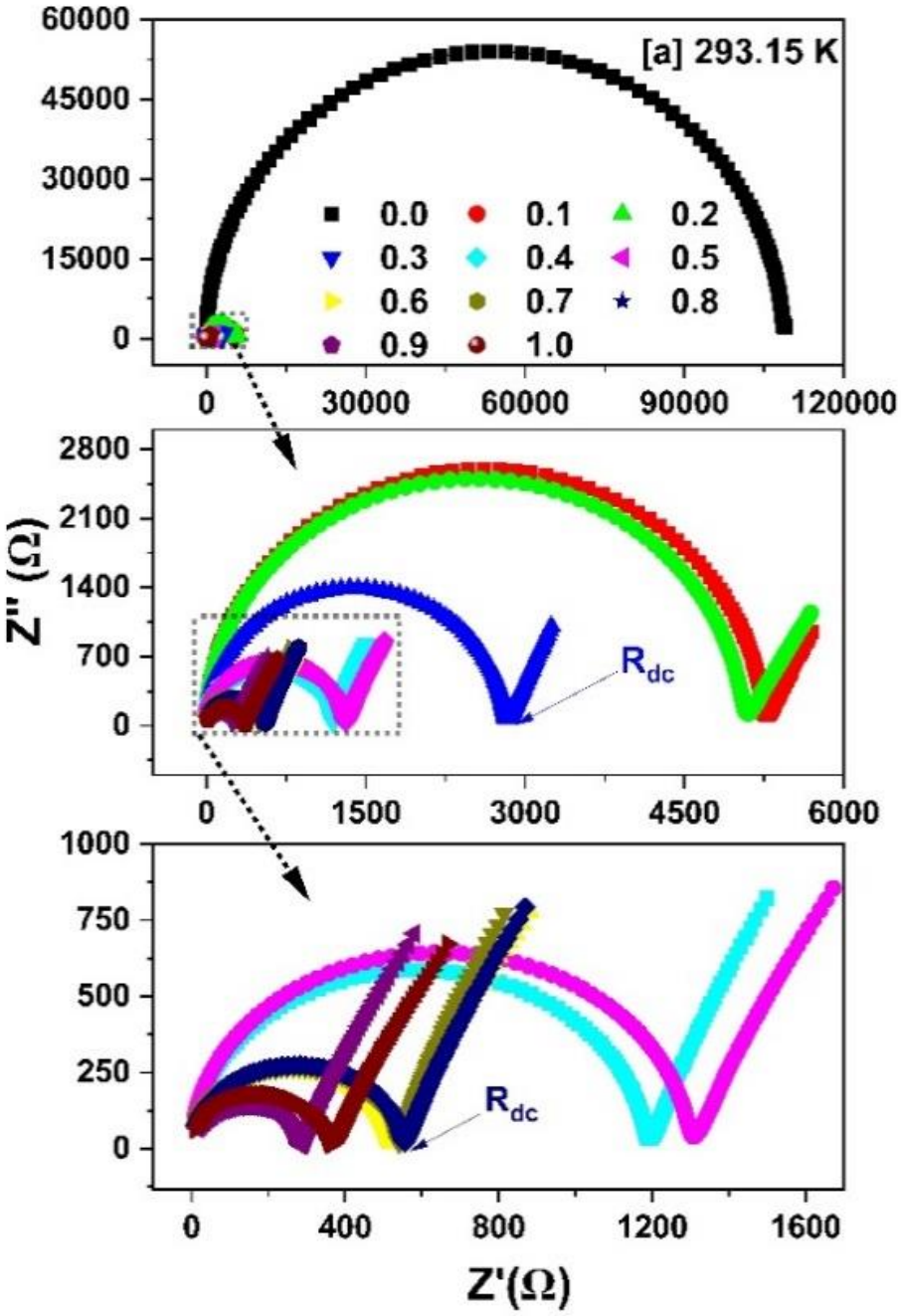

Fig. 5.11 (A) Plot of Z″ versus Z′ for all concentration range of X_A = 0.0 to X_A= 1.0 at 293.15 K.

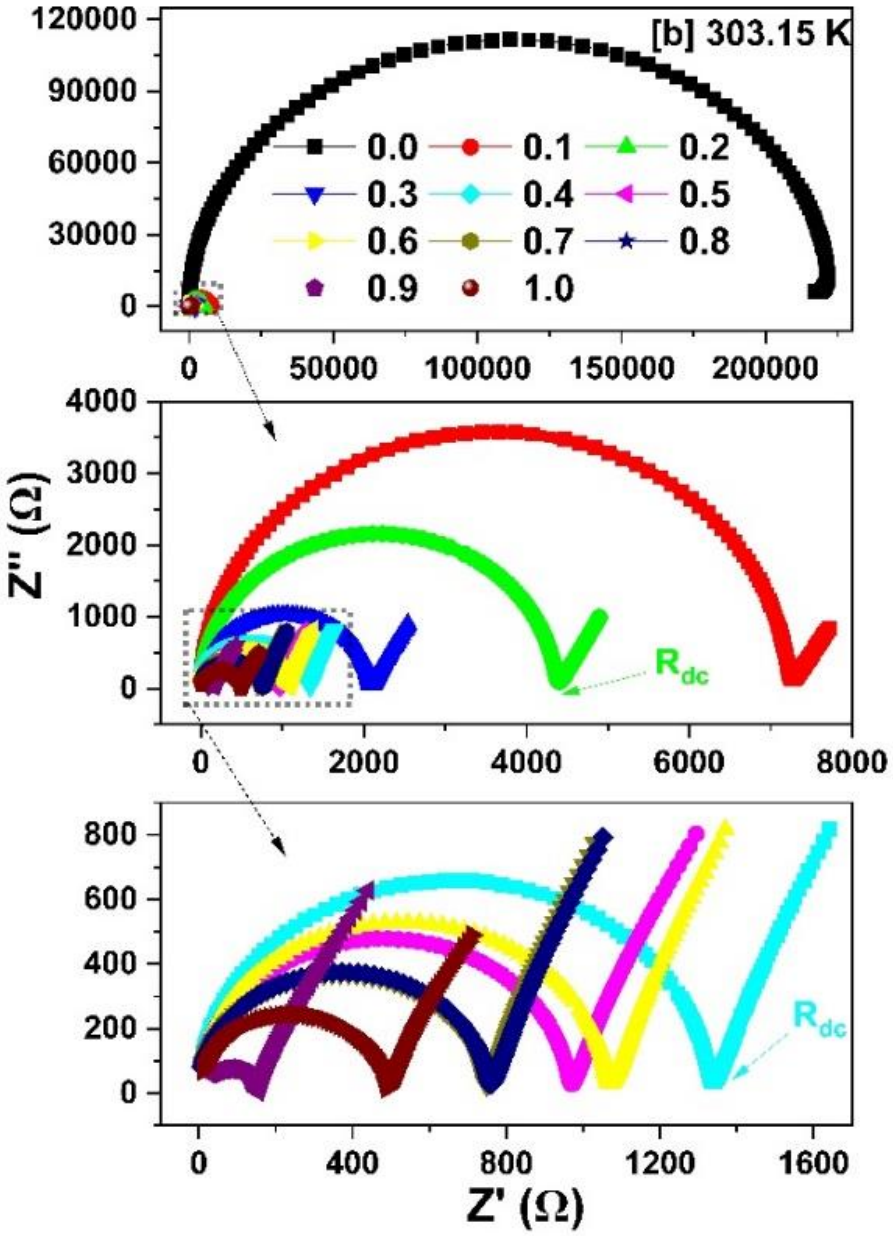

Fig. 5.11 (B) Plot of Z″ versus Z′ for all concentration range of X_A = 0.0 to X_A= 1.0 at 303.15 K.

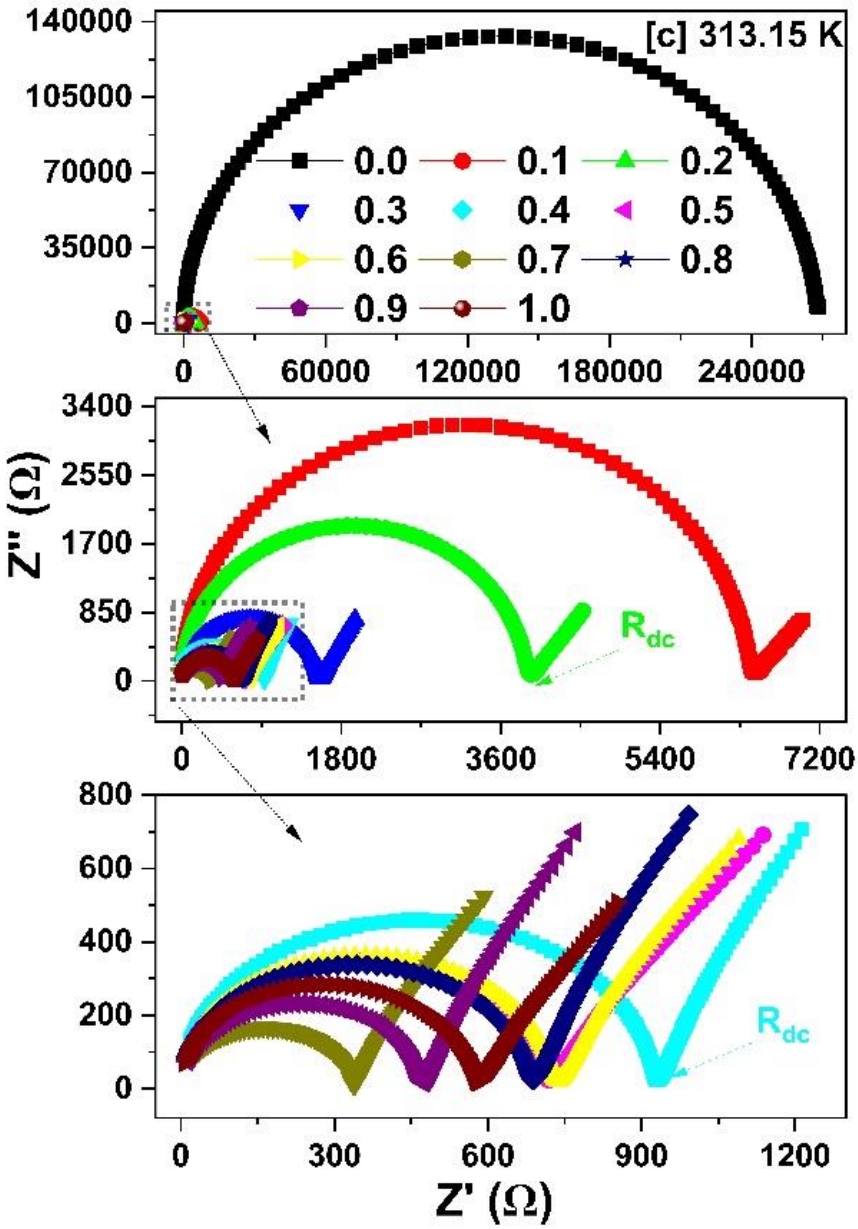

Fig. 5.11 (C) Plot of Z″ versus Z′ for all concentration range of $X_A = 0.0$ to $X_A = 1.0$ at 313.15 K.

Figure 5.11 (A), (B) and (C) depict complex impedance plane plots (Z'' versus Z') where the frequency of the experimental points increases from the right to the left side across three distinct arcs. Within the first semicircle arc corresponding to concentration $X_A = 0.0$, and the second semicircular, Debye-type arc observed for $0.1 \leq X_A \leq 0.6$, a higher

frequency is indicative of the bulk property of the material. Following this, an inclined straight line appears in the low-frequency region, signifying the dominance of the electrode polarization (EP) effect [26]. The size of the semicircular arc is noted to decrease with the increase in the concentration of DMF in the mixtures. Moreover, the plots exclusively display a Debye-type semicircular arc for the concentration range $0.7 \leq X_A \leq 1.0$. The impedance analysis of dimethylformamide (DMF) and n-Octanol reveals distinct electrical behavior, with DMF exhibiting significantly lower impedance compared to n-Octanol, consistent with their respective conductivity characteristics. The impedance plot, specifically examining the direct current resistance (R_{dc}), indicates that at 293.15 K, n-Octanol possesses a higher R_{dc} value of 108931.8 Ω, while DMF shows a markedly lower R_{dc} value of 364.85 Ω. Notably, an increase in DMF volume fraction correlates with a decreases in R_{dc} values, suggesting a concentration-dependent impact on electrical resistance. Additionally, the observed increase in R_{dc} values with rising temperature underscores the temperature sensitivity of the electrical properties in this system.

In Figure 5.12 (A), (B), and (C), tan δ, σ", M", and Z" spectra are presented on a common frequency scale for concentration values $X_A = 0.0$, $X_A = 0.5$, and $X_A = 1.0$ at different temperatures. This master plot is essential for comparing relaxation processes in the loss part spectra across different formalisms, all plotted on the same frequency scale. It serves as a key tool in confirming the appropriateness of a chosen spectrum for studying relaxation processes in dipolar liquids. This approach enables a concise and unified analysis of diverse formalisms, aiding in a clearer understanding of their behaviors in the frequency domain [24,25]. In Figure 5.12 (a), the alignment of dips in the σ" and Z" spectra at identical frequencies suggests a shared frequency for these processes, while the tanδ spectrum's peak corresponds to the frequency of the Electric Double Layers (EDLs) relaxation process [24]. Both EDLs and conductivity relaxation processes are indicated in the master curve by vertical dashed lines for different concentrations at various temperatures. Figures 5.12 (a), (b), and (c) collectively reveal a concentration-dependent shift of the EDL and conductivity peaks towards higher frequency spans, observed consistently across different temperatures. This shift is attributed to the EDL relaxation process, causing the decline in σ" and tanδ spectra, while the peak in the M" spectrum is exclusively a manifestation of the ionic relaxation process.

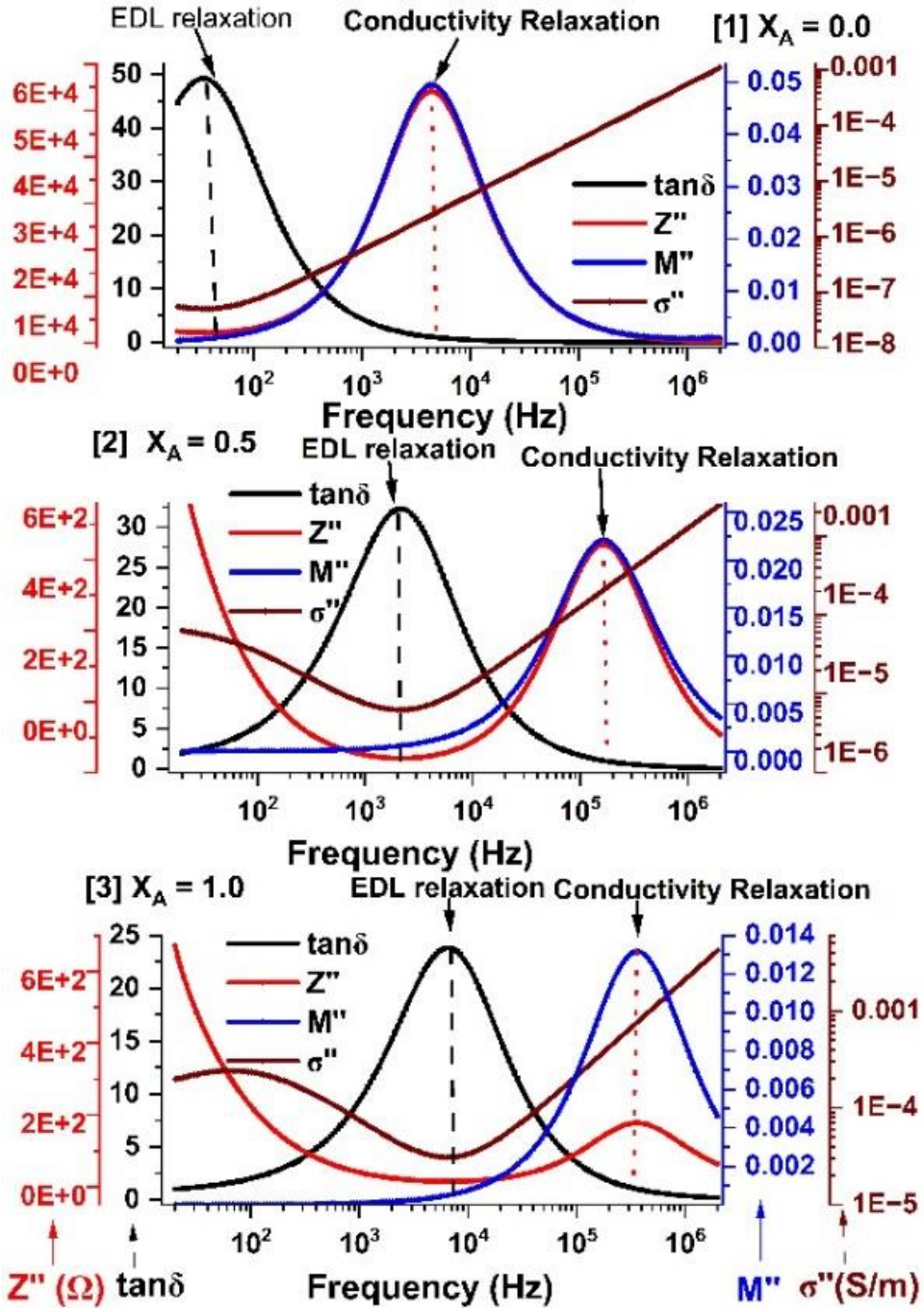

Fig. 5.12 (A) Master curves showing EDL and conductivity relaxation processes for X_A = 0.0, X_A = 0.5. and X_A = 1.0 at 293.15 K.

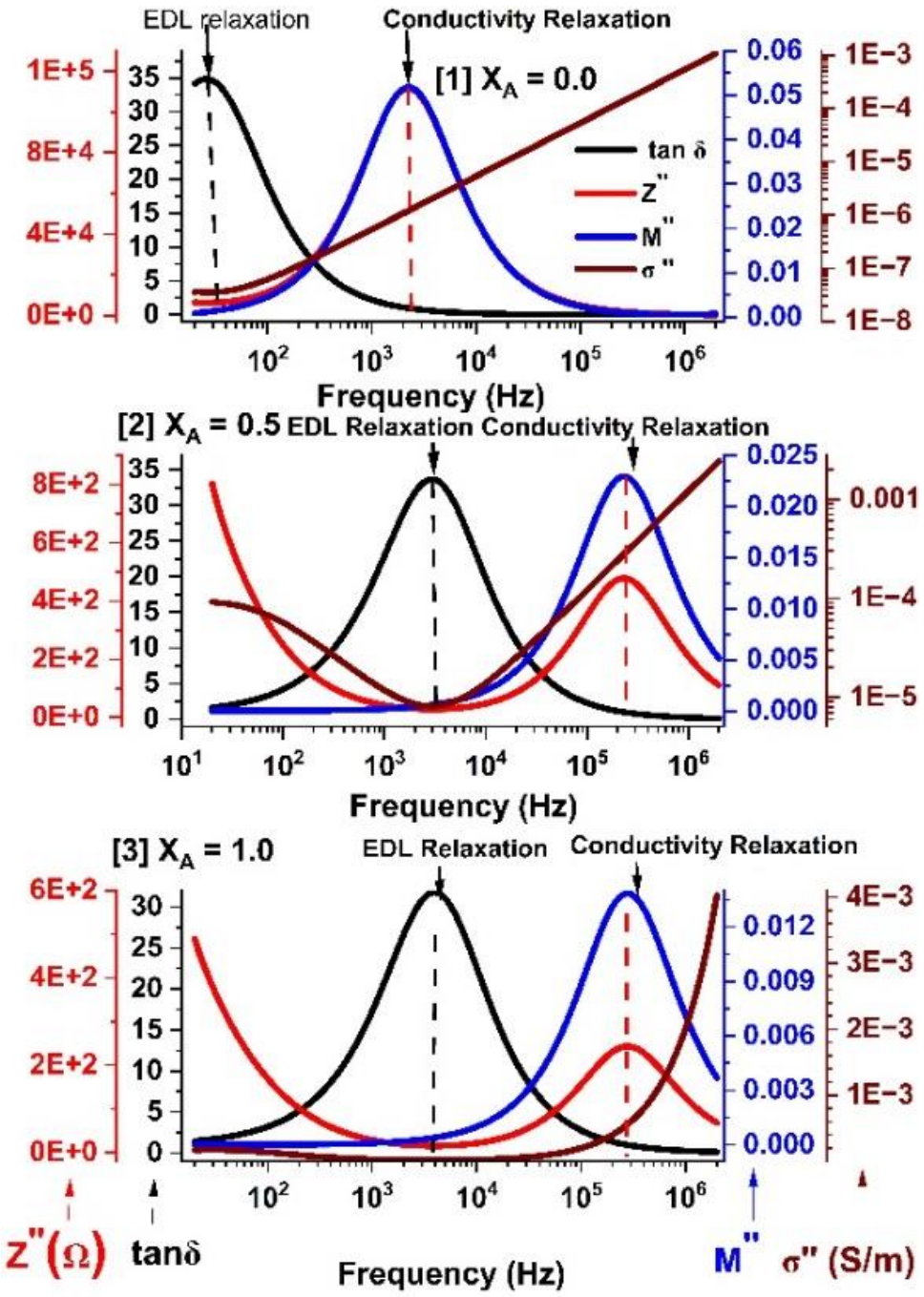

Fig. 5.12 (B) Master curves showing EDL and conductivity relaxation processes for $X_A = 0.0$, $X_A = 0.5$. and $X_A = 1.0$ at 303.15 K.

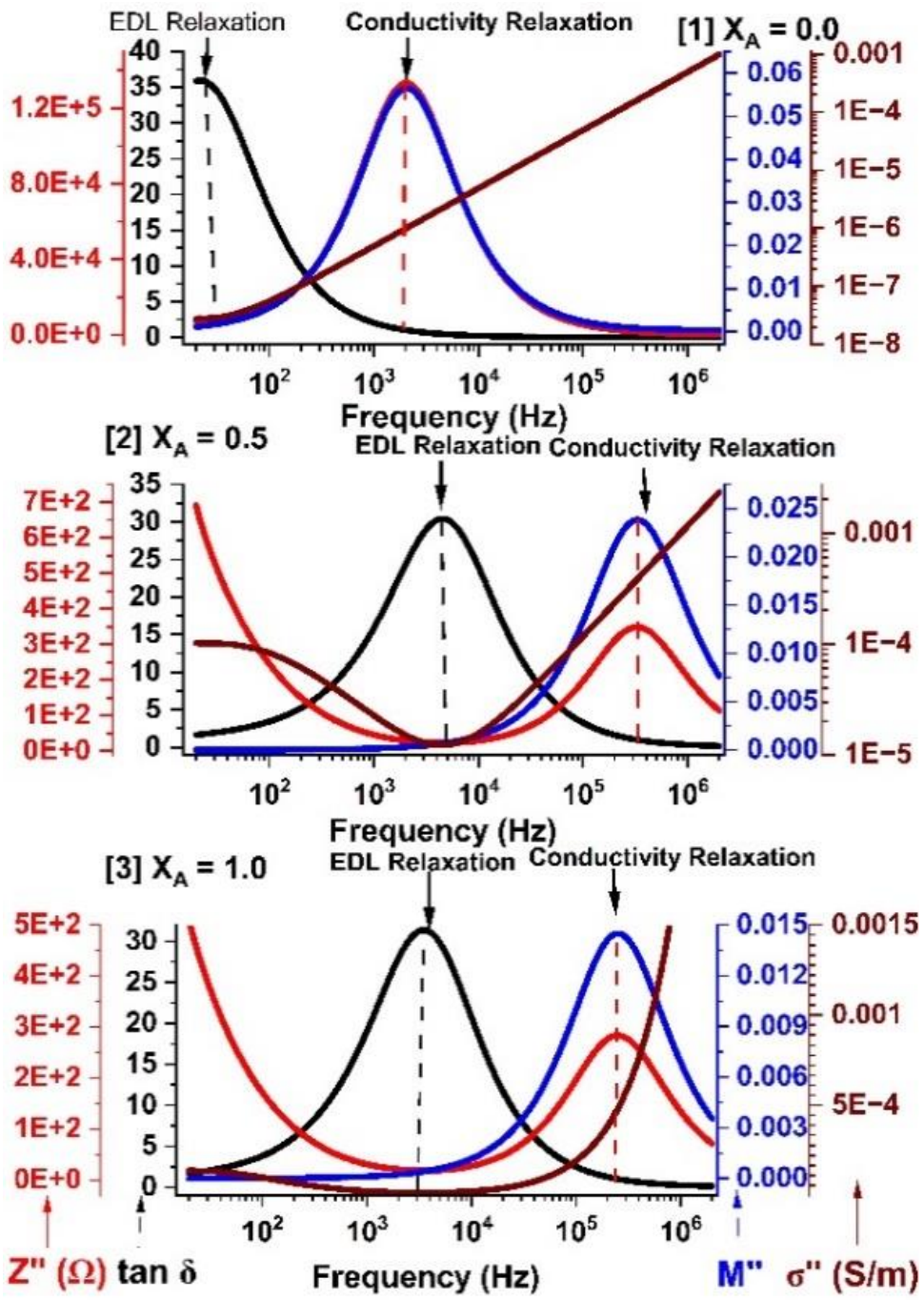

Fig. 5.12 (C) Master curves showing EDL and conductivity relaxation processes for $X_A = 0.0$, $X_A = 0.5$. and $X_A = 1.0$ at 313.15 K.

5.3.1.5 Electrochemical Impedance Spectroscopy (Nyquist plots)

Impedance spectroscopy is the method of study that is most suited for understanding the behavior of a system at different frequency ranges. Therefore, several equivalent circuit models were used to suit the analyzed system's impedance spectra. The measured sample impedance values were fitted to a three-element equivalent circuit that represented a measuring capacitive cell. Figure 5.13 (A), (B) and (C) shows the

experimental impedance for concentration range is X_A = 0.0, X_A=0.5 and X_A=1.0 data best fitted to three equivalent circuits at different temperatures. The experimental impedance data all concentration is best fitted in equivalent circuit at different temperatures. In Figure 5.13, it is observed that complex impedance (experimental and fitted) value systematically decreases with an increase in temperatures. In this figure, three element equivalent circuit is used for the fitting complex impedance data. To account for this, electrochemical impedance spectroscopy (EIS) study often uses a constant phase element (CPE) instead of a pure capacitor [41]. Complex impedance experimental fitted value equivalent circuit using equation (6) given as [42].

$$Z(f) = \frac{1+R_2Q_2\,(i2\pi f)^{\alpha_2}}{Q_2(i2\pi f)^{\alpha_2} + Q_1(i2\pi f)^{\alpha_1}\,(1+R_2Q_2\,(i2\pi f)^{\alpha_2}} \qquad (5.1)$$

Where Q (Q_1 and Q_2) is constant phase element and R_2 is resistor and α is order (α_1 = α_2 = 1). Q has units of a capacitance, i.e., μF/cm^2, and represents the capacity of the interface.

In the circuit best fit values of constant phase element (CPE) are (Q_1 and Q_2) and resistors (R_2) with geometric time constant [43,44] ($\tau_g = R_2Q_1$) for all the concentration at different temperatures are tabulated in Table 5.4. In this table observed geometric time constant values are in close agreement to the ionic relaxation time observed in Table 5.3. It is for all concentration at different temperatures. The Bode plot representation is then used for further analysis on the experimental and fitted data of complex impedance [45]. The high-frequency and low-frequency asymptotes are related to the parameters of a model based on a three-element circuit. In Figure 5.14 (a), (b) and (c) the Bode plots for pure n-octanol +DMF system for concentration X_A = 0.0 and X_A = 0.5 at different temperatures show low and high frequency asymptotes, along with the importance associated with those asymptotes. These asymptotes are shown by horizontal dotted lines.

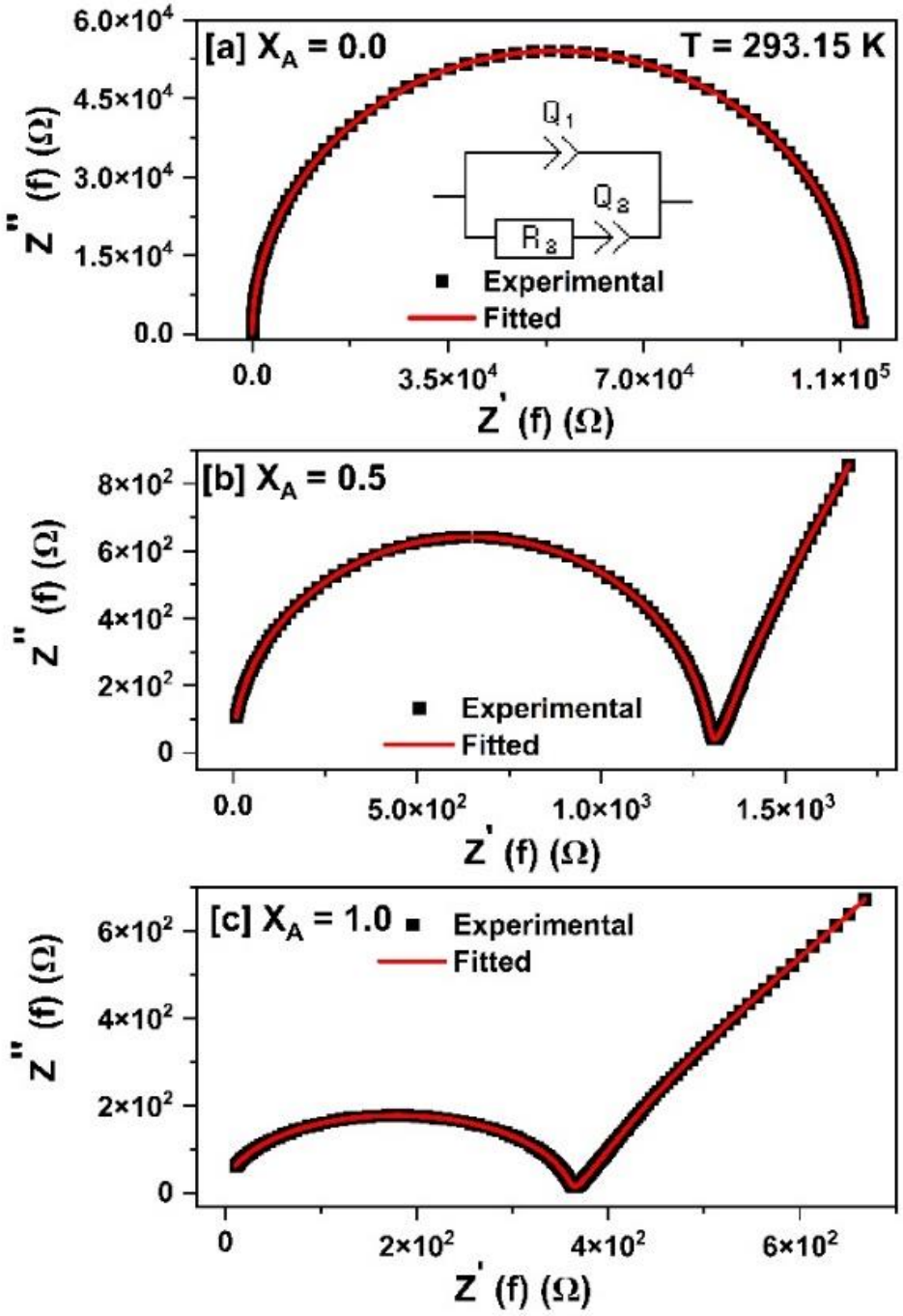

Fig. 5.13 (A) Experimental data points and fitted data points of complex impedance spectra with a three-element equivalent RC circuit for concentration $X_A = 0.0$, $X_A = 0.5$. and $X_A = 1.0$ at 293.15 K.

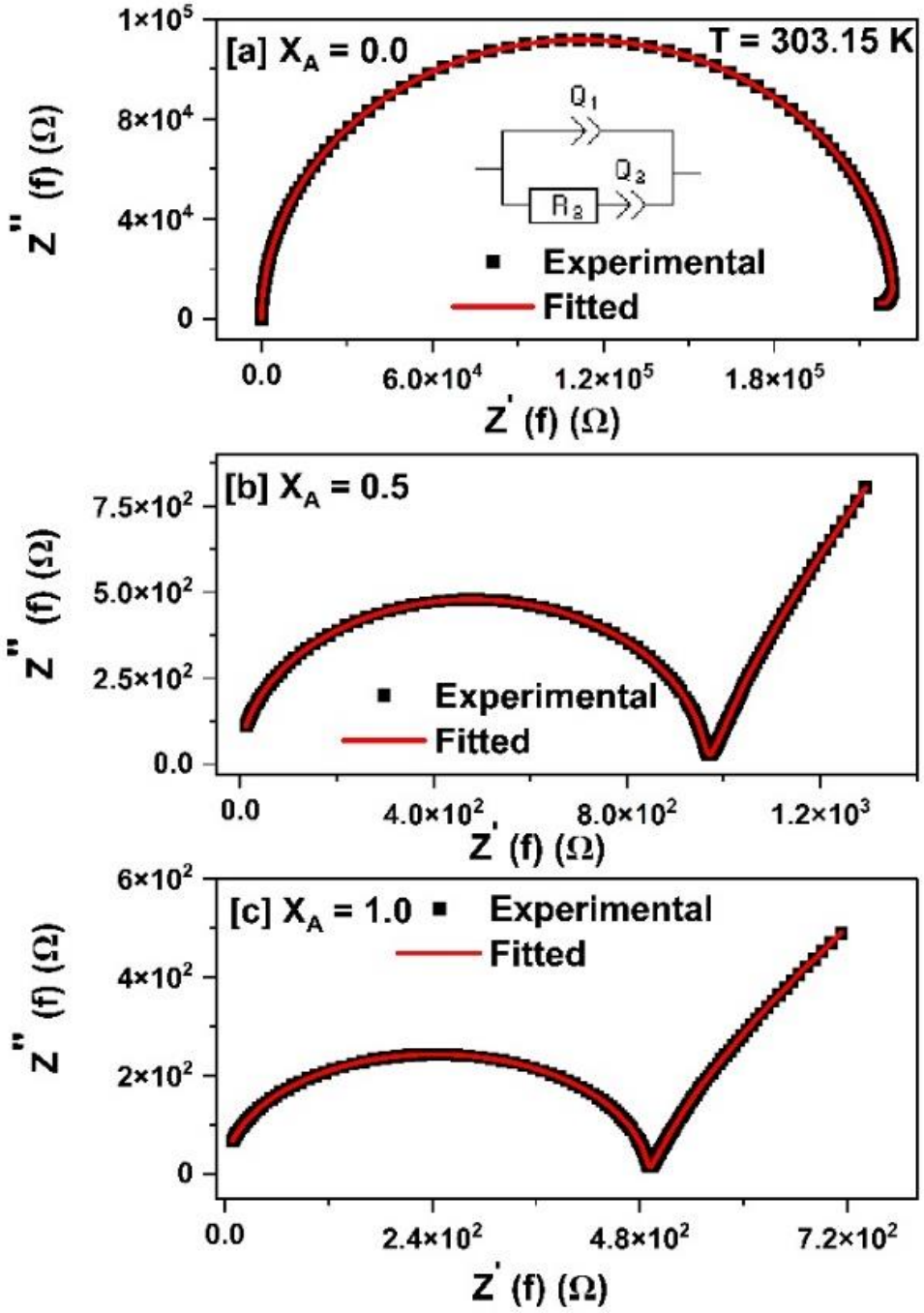

Fig. 5.13 (B) Experimental data points and fitted data points of complex impedance spectra with a three-element equivalent RC circuit for concentration $X_A = 0.0$, $X_A = 0.5$. and $X_A = 1.0$ at 303.15 K.

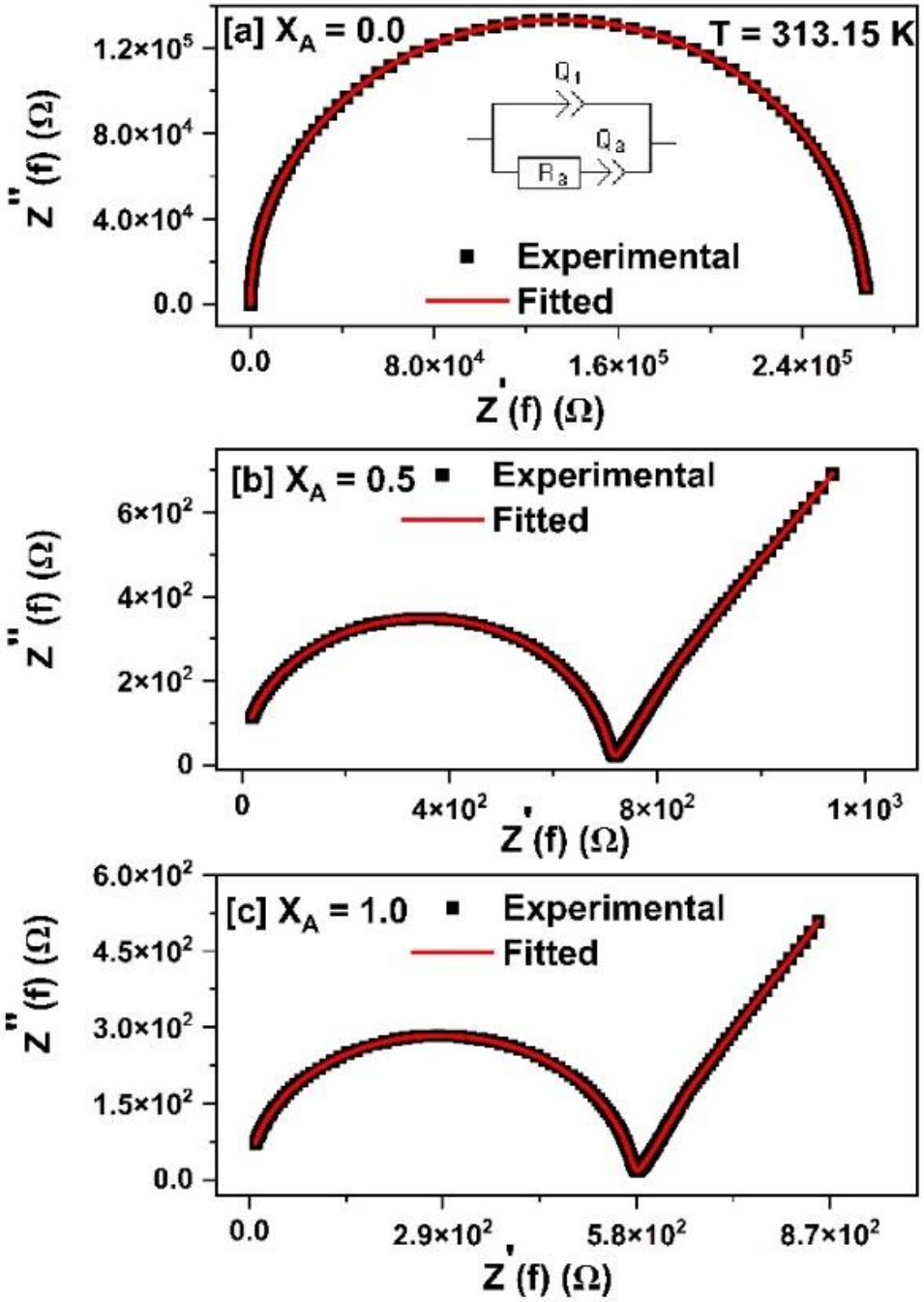

Fig. 5.13 (C) Experimental data points and fitted data points of complex impedance spectra with a three-element equivalent RC circuit for concentration $X_A = 0.0$, $X_A = 0.5$. and $X_A = 1.0$ at 313.15 K.

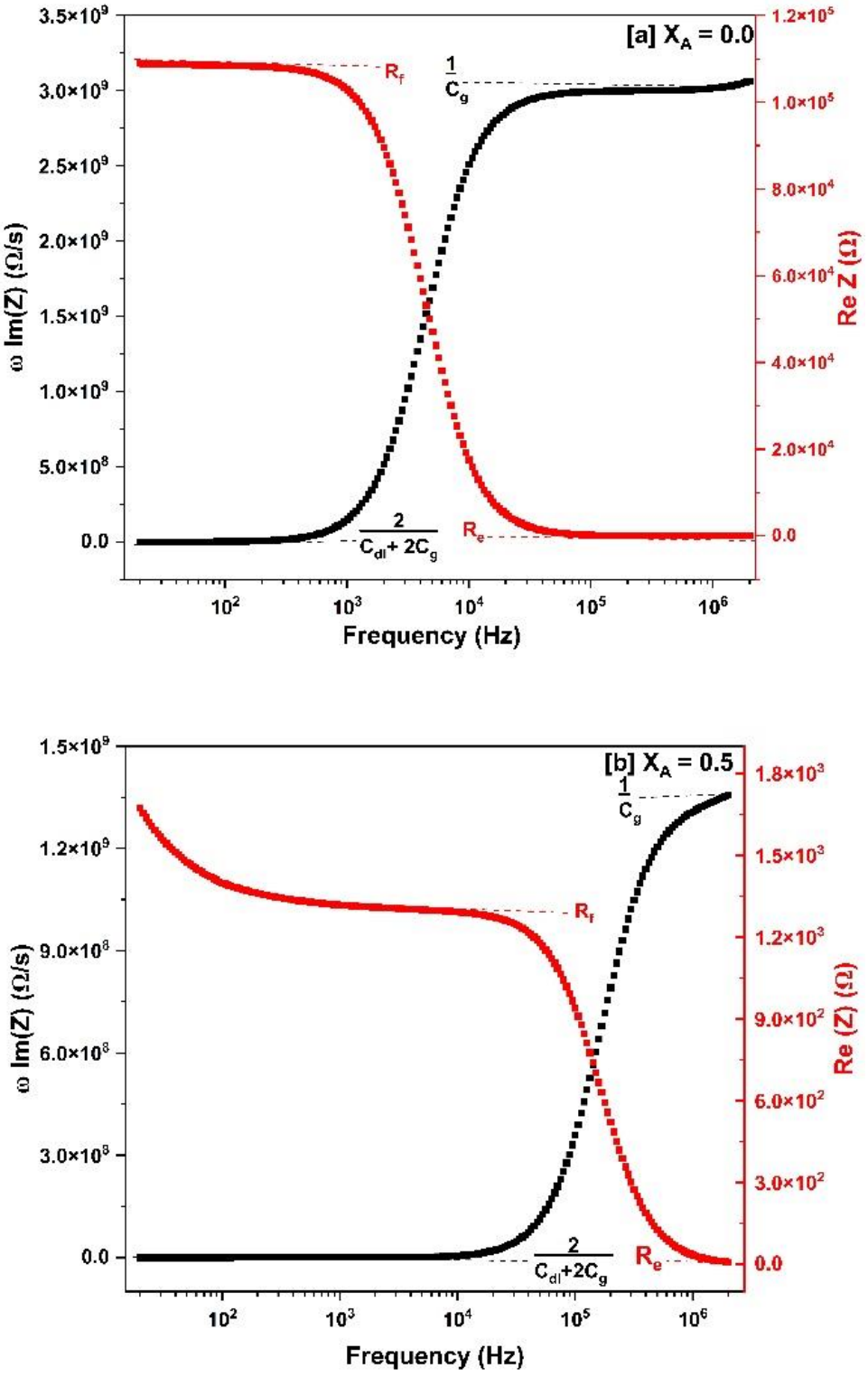

Fig. 5.14 (A) Bode plot analysis of the complex impedance for (A)X_A= 0.00 and (B)X_A = 0.5 at 293.15 K.

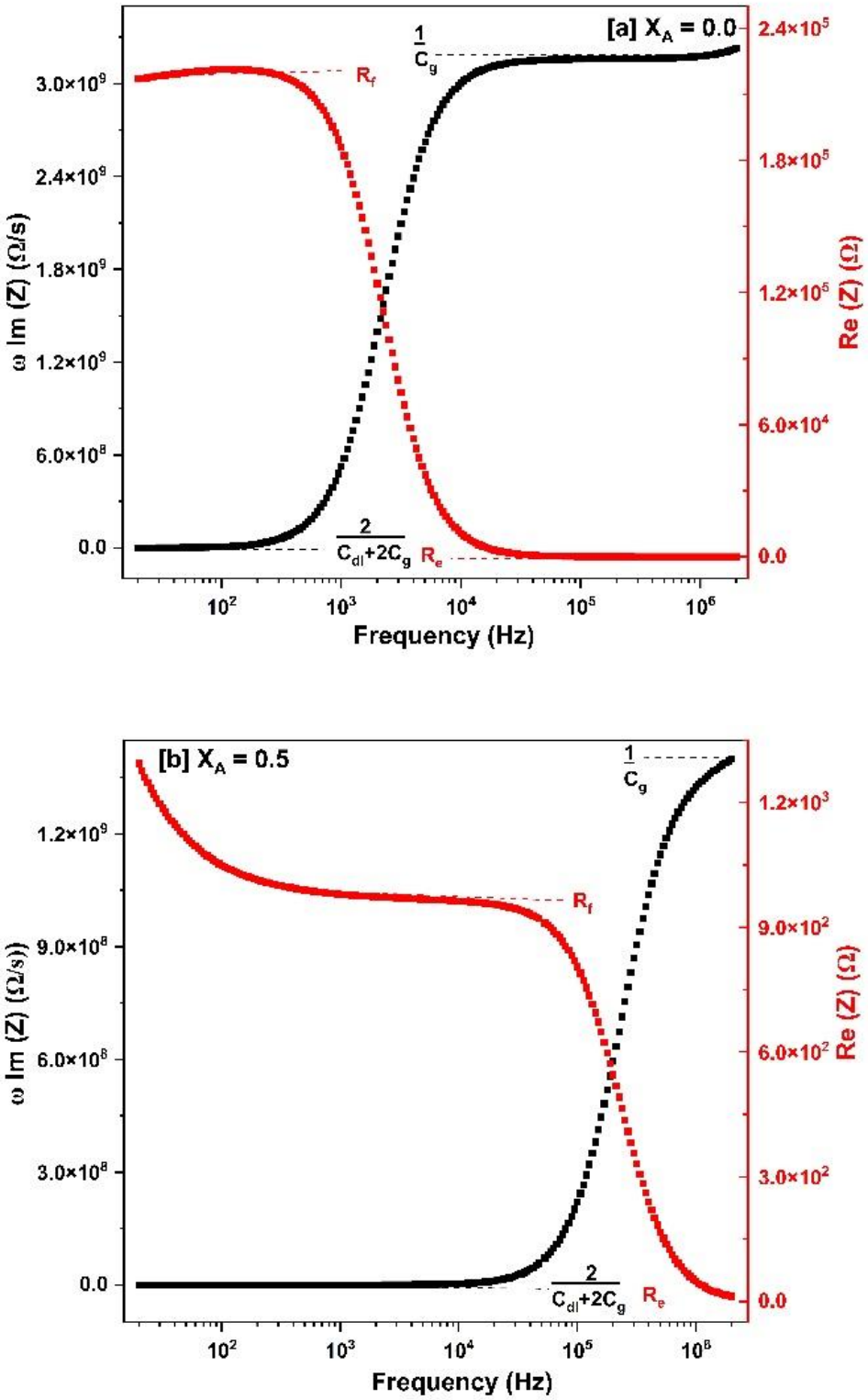

Fig. 5.14 (B) Bode plot analysis of the complex impedance for (A)X_A= 0.00 and (B)X_A = 0.5 at 303.15 K.

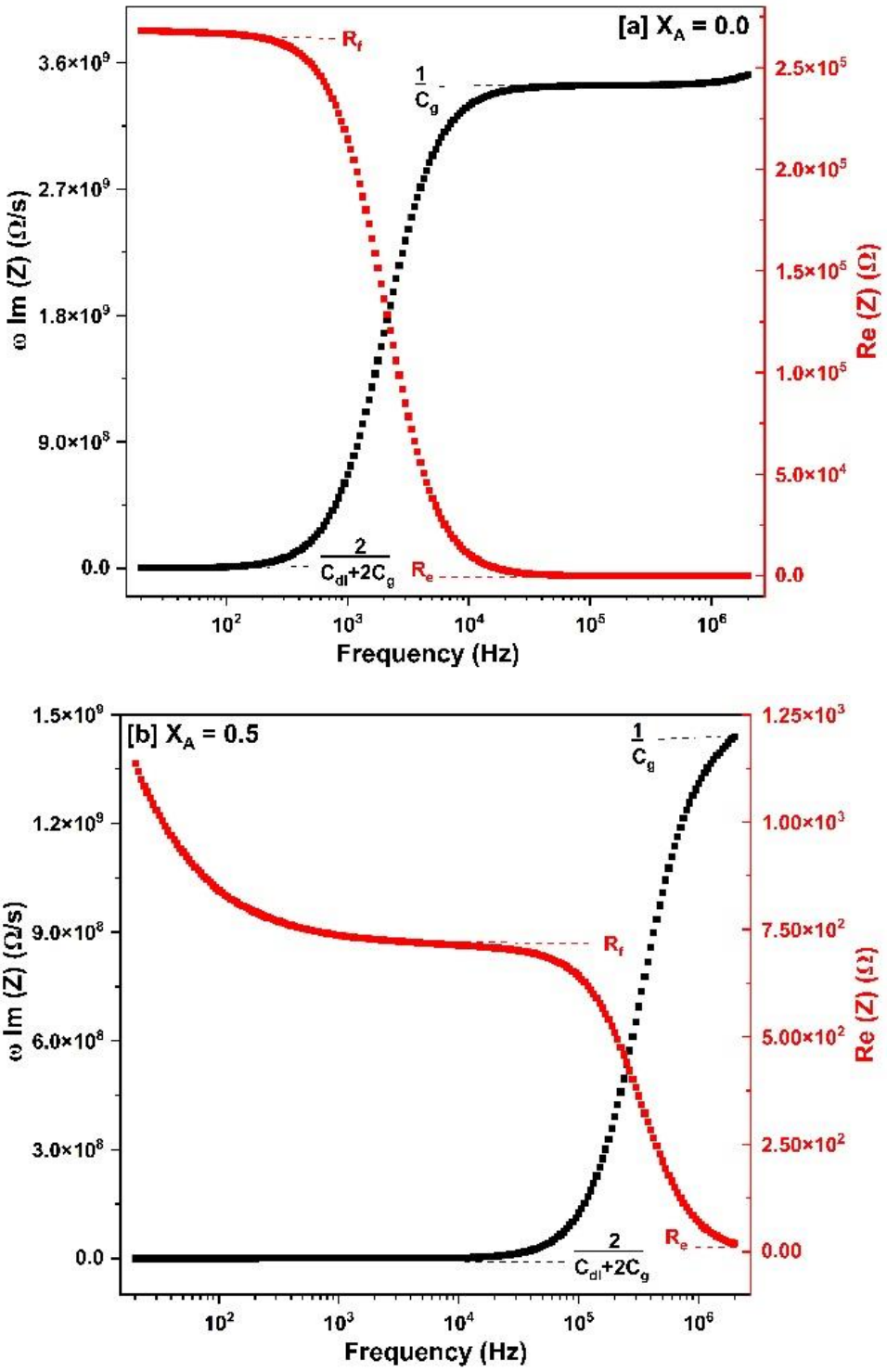

Fig. 5.14 (C) Bode plot analysis of the complex impedance for (A)X_A= 0.00 and (B)X_A = 0.5 at 313.15 K.

In this Figure 5.14 (A), (B) and (C) the low and high frequency asymptotes are represented in the form fluid resistance (R_f), geometric capacitance (C_g), double – layer capacitance (C_{dl}) and resistance of external circuit (Re). Values of C_g =0.3266 nf, C_{dl} = 6.55 μF, R_f = 108932 Ω and R_e=2.88 Ω for pure n-Octanol at 293.15 K temperature are

observed. In this observation the bode plot in fluid resistance value nearly equally to R_{dc} value and geometric capacitance (C_g) values are nearly equal to capacitance phase element (CPE) parameters (Q_1) values for all concentration at different temperatures.

Table 5.4 Fitted parameters of three element equivalent RC circuit and geometric time constant (τ_g) for all concentration at different temperatures.

X_A	Q_1 (μ.F.s)	Q_2 (μ.F.s)	R_2 (MΩ)	τ_g (μs)	τ_{dl} (μs)
T= 293.15 K					
0.0	340.8	9.306	0.10840	36.94	1.0088
0.1	402.6	29.83	0.00524	2.11	0.1562
0.2	479	29.2	0.00504	2.42	0.1472
0.3	581.4	26.18	0.00281	1.63	0.0735
0.4	681	26.79	0.00118	0.80	0.0317
0.5	781.5	28.88	0.00130	1.01	0.0374
0.6	865.9	32.8	0.00051	0.44	0.0168
0.7	944.9	25.91	0.00053	0.51	0.0139
0.8	1068	28.57	0.00055	0.58	0.0156
0.9	1155	33.26	0.00028	0.32	0.0093
1.0	1304	38.09	0.00036	0.47	0.0137
T= 303.15 K					
0.0	321	1.528	0.22196	71.25	0.3391
0.1	377	44.53	0.00721	2.72	0.3209
0.2	467	33.8	0.00436	2.03	0.1473
0.3	553.7	32.37	0.00207	1.15	0.0671
0.4	620.2	27.3	0.00133	0.82	0.0362
0.5	742.7	28.3	0.00096	0.71	0.0272
0.6	814.8	26.63	0.00106	0.87	0.0283
0.7	939.6	26.88	0.00074	0.70	0.0200
0.8	1036	26.93	0.00075	0.78	0.0203
0.9	1106	37.03	0.00015	0.16	0.0055
1.0	1173	50.78	0.00006	0.07	0.0029
T= 313.15 K					
0.0	295.7	3.467	0.26716	79.00	0.9262

0.1	359.2	67.11	0.00639	2.30	0.4290
0.2	446.2	53.51	0.00389	1.73	0.2079
0.3	549.5	40.27	0.00154	0.85	0.0620
0.4	618.4	31.99	0.00092	0.57	0.0295
0.5	732.8	50.08	0.00071	0.52	0.0354
0.6	813.9	41.65	0.00073	0.59	0.0302
0.7	892.2	49.48	0.00033	0.30	0.0165
0.8	1014	30.96	0.00068	0.69	0.0211
0.9	1101	33.52	0.00047	0.51	0.0156
1.0	1089	79.09	0.00004	0.04	0.0029

Klein's model [46] was utilized to determine parameters such as ion buildup thickness, ion mobility, mobile ion concentration, and ion diffusivity, as described in Chapter 3. These parameters were calculated using Equations (3.11) to (3.14) for the concentration range $0.00 \leq X_A \leq 1.0$. The calculated values are summarized in Table 5.5. The observed table 5.5 Octanol has the lowest Debye layer, DMF has the highest, and mixtures have a layer which lies in between these two values. Mobile ion concentration is Highest in octanol, and it decreases with increase in concentration of DMF. Because of the low molecular size, lowest density, and low viscosity of octanol may be responsible for all variation in such parameters. The ion mobility found to increases with increasing DMF concentration in the mixture and reaches its maximum it becomes 90% concentration. This shows that at this concentration, molecular structures are produced that allow ions to system has evolved across the medium.

Table 5.5 Calculated values of Debye length (λ_D), Ion mobility (μ), Mobile ion concentration (P_0), and ion diffusivity (D) for the binary mixtures of n-Octanol and N, N-Dimethylformamide at different temperatures.

X_A	λ_D(nm)	μ (m^2/vs)	P_0 (m^{-3})	D (m^2/s)
T= 293.15 K				
0.0	7.81	6.79E-14	2.30E+26	1.71E-15
0.1	6.93	9.50E-13	3.39E+26	2.39E-14
0.2	9.56	1.61E-12	2.07E+26	4.07E-14
0.3	10.72	2.86E-12	2.10E+26	7.22E-14
0.4	9.60	4.84E-12	2.94E+26	1.22E-13

0.5	13.58	7.71E-12	1.68E+26	1.94E-13
0.6	11.16	1.17E-11	2.80E+26	2.94E-13
0.7	18.93	2.82E-11	1.11E+26	7.12E-13
0.8	21.46	3.23E-11	9.48E+25	8.16E-13
0.9	14.81	2.74E-11	2.18E+26	6.91E-13
1.0	22.39	4.43E-11	1.05E+26	1.11E-12
T= 303.15 K				
0.0	14.22	1.09E-13	7.19E+25	2.85E-15
0.1	5.83	4.87E-13	4.80E+26	1.27E-14
0.2	8.02	1.30E-12	2.96E+26	3.40E-14
0.3	9.23	3.07E-12	2.64E+26	8.02E-14
0.4	11.38	5.87E-12	2.16E+26	1.53E-13
0.5	13.38	1.02E-11	1.71E+26	2.67E-13
0.6	14.80	9.93E-12	1.60E+26	2.59E-13
0.7	17.00	1.65E-11	1.37E+26	4.31E-13
0.8	24.09	2.95E-11	7.57E+25	7.71E-13
0.9	14.10	4.52E-11	2.47E+26	1.18E-12
1.0	15.74	1.68E-11	2.05E+26	4.39E-13
T= 313.15 K				
0.0	10.54	5.47E-14	1.16E+26	1.48E-15
0.1	4.93	4.01E-13	6.54E+26	1.08E-14
0.2	6.51	9.86E-13	4.37E+26	2.66E-14
0.3	8.00	2.98E-12	3.66E+26	8.03E-14
0.4	7.53	3.95E-12	4.62E+26	1.06E-13
0.5	11.62	1.05E-11	2.24E+26	2.85E-13
0.6	9.34	5.73E-12	4.02E+26	1.55E-13
0.7	14.11	2.47E-11	2.04E+26	6.65E-13
0.8	17.98	1.79E-11	1.38E+26	4.82E-13
0.9	19.27	2.74E-11	1.31E+26	7.39E-13
1.0	13.55	1.08E-11	2.72E+26	2.90E-13

5.3.2 Dielectric relaxation spectroscopy in the Higher Frequency Range 200 MHz to 20 GHz

5.3.2.1 Complex dielectric permittivity spectra

Figure 5.15 (A & B) illustrates the complex permittivity $\varepsilon^*(f) = \varepsilon' - j\varepsilon''$ of n-Octanol and N, N-Dimethylformamide (DMF) mixtures across all concentrations (0.0 →1.0) and at different temperatures (293.15 K, 303.15 K and 313.15K) as a function of frequency (200 MHz to 20 GHz). In Figure 5.15 (A), (B) and (C) solid lines show the Cole-Cole fitted values of the permittivity spectra using LEVMW software and symbol represents the experimental values of the real part of permittivity at different temperatures. The real part of the dielectric permittivity ε′ remains nearly constant up to a certain frequency, beyond which it decreases with increasing frequency. This behavior suggests that not all the energy imparted by the applied electric field is utilized for dipole orientation [47,48]. As the concentration of n-Octanol increases, the real part of the dielectric permittivity decreases.

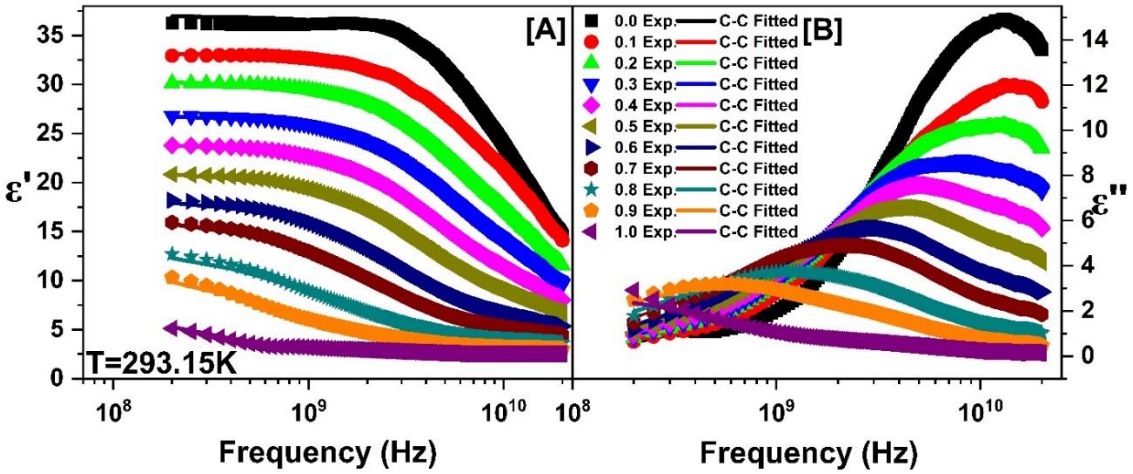

Fig.5.15 (A) Variation of [A] real part of permittivity (ε′) [B] imaginary part of permittivity (ε′′) against frequency at different concentration of n-Octanol in binary mixtures Solid line represent Cole-Cole (C-C) Fitted at 293.15 K.

Furthermore, observed from Fig. 5.15 (A) that the dielectric constant (ε′) values decreases with increase in frequency monotonically as the concentration of n-octanol increases in the binary liquid mixtures. Besides, the dielectric constant (ε′) of n-octanol exhibited frequency-independent behavior across various concentrations within the range of 200 MHz–3 GHz. However, beyond this range, there was a notable decrease

in the dielectric constant with increasing frequency. This decrease in ε′ beyond 3 GHz, extending up to 20 GHz, can be attributed to the phase lag between dipolar orientation and the alternating electric field, particularly pronounced at frequencies exceeding 20 GHz [49,50].

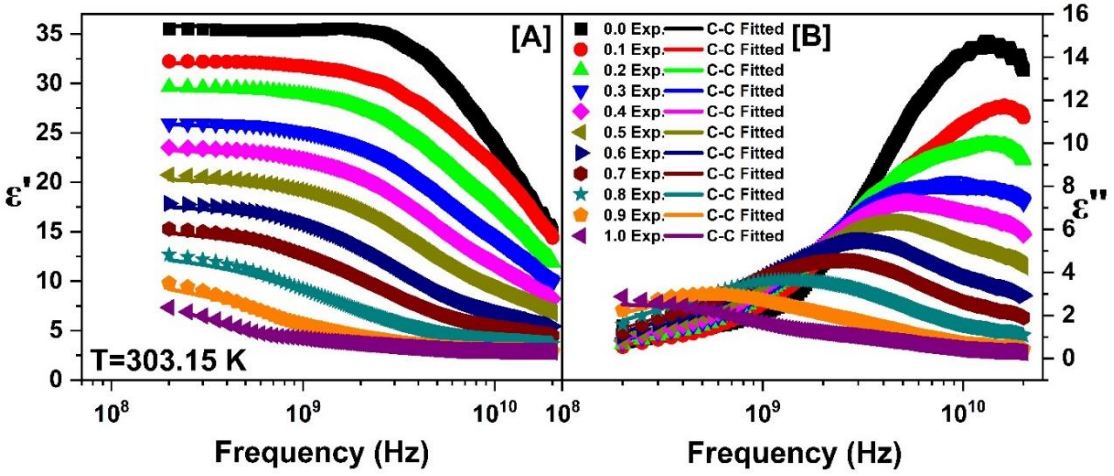

Fig.5.15 (B) Variation of [A] real part of permittivity (ε′) [B] imaginary part of permittivity (ε′′) against frequency at different concentration of n-Octanol in binary mixtures Solid line represent Cole-Cole (C-C) Fitted at 303.15 K.

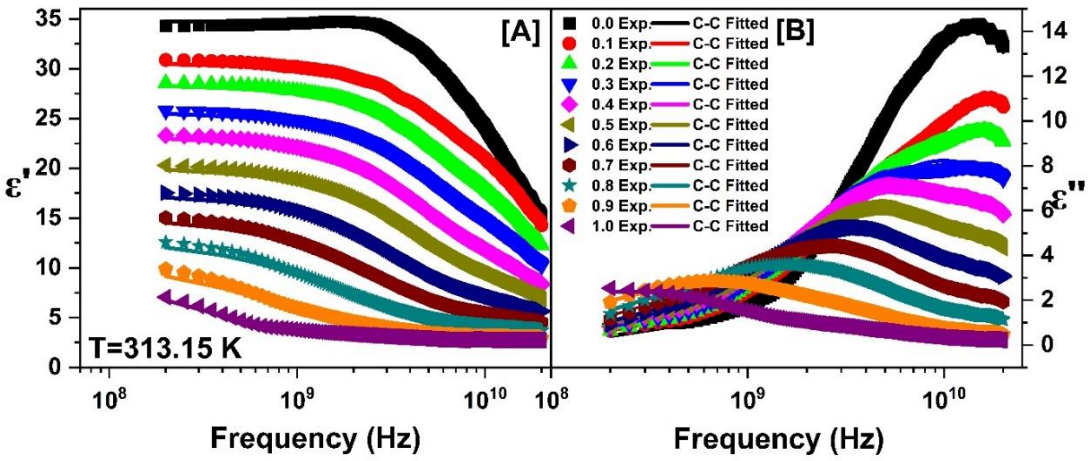

Fig.5.15 (C) Variation of [A] real part of permittivity (ε′) [B] imaginary part of permittivity (ε′′) against frequency at different concentration of n-Octanol in binary mixtures Solid line represent Cole-Cole (C-C) Fitted at 313.15 K.

Fig. 5.15 (B) presents the imaginary part of the permittivity ε′′, where a peak is observed for all concentrations within the frequency range of approximately 0.2 GHz to 1 GHz. This peak signifies "dipolar relaxation," a process during which orientation polarization

of a substance takes a definite time to reach equilibrium after a change in the applied electric field [47]. The peak values shift toward lower frequencies as the concentration of n-Octanol increases, indicating the formation of intermolecular hydrogen bonds between n-Octanol and DMF. Due to the hydroxyl group in n-Octanol's molecular structure and the intramolecular linked clusters formed by the (O-H ····O) linkage, n-Octanol exhibits a longer relaxation time (769.34 ps). In contrast, DMF has a shorter relaxation time (12.47 ps), reflecting its rigid and non-associative nature at 303.15 K. Additionally, a significant deviation is observed in the fitted data at lower frequencies compared to the experimental data, which is attributed to the dc ionic conduction loss effect not accounted for during the fitting process. The deviation in the higher frequency region suggests the onset of a higher frequency dielectric relaxation process. Before analyzing the dielectric parameters and hetero-molecular conformations of the mixed solvents under study, it is crucial to first examine the dielectric behavior and structural conformations of the pure liquids. The ε′ and ε′′ parts of the complex permittivity (ε*f) spectra for binary mixtures at different concentrations (0.0→1.0) are analyzed using the Cole-Cole (CC) model with a CNLS fitting program. Table 5.6 presents key results at different temperatures, including the high-frequency dielectric constant (ε_∞), dielectric strength ($\Delta\varepsilon$), relaxation time (τ_d), and shape parameter (α). It shows that as the concentration of n-Octanol in the (n-Octanol + DMF) mixtures increases, the high-frequency dielectric constant ($\varepsilon\infty$) decreases, while the dielectric strength ($\Delta\varepsilon$) also decreases and the relaxation time (τ) increases with increases in temperatures. These parameters are influenced by factors such as viscosity, density, temperature, and molecular structure.

Table 5.6 The CNLS fitting parameters such as ε_∞, $\Delta\varepsilon$, τ, and α are determined for different mole fractions of n-Octanol in n-Octanol + DMF mixtures at different temperatures.

X	ε_∞	$\Delta\varepsilon$	τ (ps)	α
T= 293.15 K				
0.0000	5.11 ± (2.53)	31.88 ± (0.53)	12.93 ± (0.45)	0.95 ± (0.37)
0.0516	4.71 ± (3.53)	28.55 ± (0.51)	12.66 ± (0.95)	0.89 ± (0.34)
0.1090	4.31 ± (2.93)	26.14 ± (0.45)	15.73 ± (0.84)	0.85 ± (0.36)
0.1733	4.46 ± (2.56)	22.56 ± (0.50)	19.43 ± (0.91)	0.84 ± (0.46)
0.2459	4.26 ± (2.03)	19.86 ± (0.48)	24.66 ± (0.84)	0.82 ± (0.49)

0.3285	4.08 ± (1.56)	17.19 ± (0.51)	33.61 ± (0.83)	0.81 ± (0.53)
0.4232	3.85 ± (1.16)	14.63 ± (0.58)	48.92 ± (0.96)	0.80 ± (0.57)
0.5330	3.57 ± (0.76)	12.96 ± (0.64)	76.99 ± (1.14)	0.80 ± (0.52)
0.6618	3.14 ± (0.56)	10.34 ± (0.88)	134.78 ± (1.74)	0.78 ± (0.56)
0.8149	2.87 ± (0.35)	8.65 ± (1.12)	252.48 ± (2.13)	0.81 ± (0.45)
1.0000	2.44 ± (0.64)	6.84 ± (8.59)	1072.80 ± (1.46)	0.78 ± (1.16)
T= 303.15 K				
0.0000	5.79 ± (8.00)	30.01 ± (1.30)	12.47 ± (2.09)	0.98 ± (0.82)
0.0516	4.61 ± (4.73)	27.56 ± (0.69)	11.61 ± (1.29)	0.89 ± (0.42)
0.1090	4.44 ± (3.64)	25.17 ± (0.58)	14.49 ± (1.11)	0.86 ± (0.44)
0.1733	4.29 ± (3.04)	21.81 ± (0.58)	17.86 ± (1.09)	0.83 ± (0.51)
0.2459	4.27 ± (2.38)	19.26 ± (0.56)	22.52 ± (1.00)	0.82 ± (0.54)
0.3285	4.19 ± (1.87)	16.46 ± (0.60)	30.35 ± (1.00)	0.82 ± (0.62)
0.4232	3.84 ± (1.28)	14.17 ± (0.60)	44.47 ± (0.98)	0.80 ± (0.60)
0.5330	3.56 ± (0.92)	11.96 ± (0.69)	66.53 ± (1.20)	0.80 ± (0.61)
0.6618	3.15 ± (0.62)	9.99 ± (0.87)	118.93 ± (1.68)	0.79 ± (0.59)
0.8149	2.78 ± (0.26)	7.82 ± (1.41)	244.15 ± (2.52)	0.82 ± (0.57)
1.0000	2.64 ± (0.34)	6.34 ± (2.38)	769.34 ± (5.21)	0.62 ± (1.04)
T= 313.15 K				
0.0000	6.78 ± (0.57)	27.97 ± (1.14)	12.25 ± (1.78)	1.00 ± (0.68)
0.0516	3.25 ± (6.77)	27.37 ± (072)	10.26 ± (1.39)	0.85 ± (0.41)
0.1090	4.11 ± (4.57)	24.33 ± (0.70)	12.87 ± (1.37)	0.84 ± (0.49)
0.1733	3.99 ± (3.60)	21.74 ± (0.62)	15.92 ± (1.22)	0.82 ± (0.52)
0.2459	4.14 ± (2.49)	19.15 ± (0.56)	21.45 ± (1.02)	0.82 ± (0.54)
0.3285	4.05 ± (1.92)	16.16 ± (0.57)	28.13 ± (0.97)	0.81 ± (0.60)
0.4232	3.90 ± (1.42)	13.58 ± (0.61)	38.66 ± (1.00)	0.81 ± (0.63)
0.5330	3.55 ± (0.97)	11.58 ± (0.70)	62.55 ± (1.20)	0.79 ± (0.64)
0.6618	3.20 ± (0.67)	9.68 ± (0.85)	104.06 ± (1.61)	0.79 ± (0.61)
0.8149	2.80 ± (0.43)	7.69 ± (1.22)	224.60 ± (2.36)	0.81 ± (0.55)
1.0000	2.60 ± (0.44)	5.89 ± (2.46)	720.52 ± (4.78)	0.70 ± (0.76)

* Numbers in brackets represent uncertainties in the last significant digits, as determined by the least squares fit method (CNLS). For instance, 31.88 (0.53) indicates 31.88 ± 0.53%.

5.3.2.2 dielectric relaxation strength and relaxation time

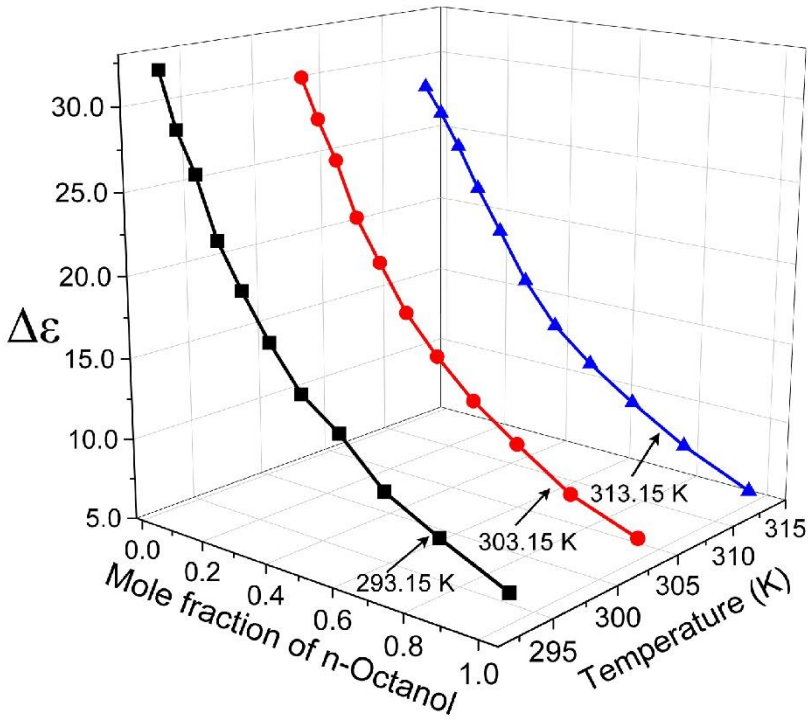

Fig. 5.16. Plots of dielectric relaxation strength (Δε) against mole fraction of n-Octanol in DMF at different temperatures.

The complex dielectric data were analyzed using the CNLS method with the LEVMW software, which helped determine key dielectric parameters like relaxation strength (Δε) and relaxation time (τ_d). Figure 5.16 illustrates the variation of dielectric relaxation strength (Δε) with the mole fraction of n-Octanol in the mixture at different temperatures. The results indicate that Δε decreases as the concentration of DMF increases, and this trend becomes more pronounced with increasing temperature. Furthermore observed studied temperature variation in dielectric relaxation strength is nonlinear, likely due to the interaction between n-Octanol and DMF molecules. Dielectric relaxation strength for DMF is 30.01, while for n-Octanol, it is 6.34, meaning the Δε for DMF is about 4.73 times higher than for n-Octanol at 303.15 K temperature. As the mole fraction of n-Octanol (X) increases, the dielectric relaxation strength decreases, indicating that a small concentration of the -OH group (n-Octanol molecules) affects the rapid reduction in Δε values in the mixtures. This decrease is faster in the DMF-rich region and slower in the n-Octanol rich region.

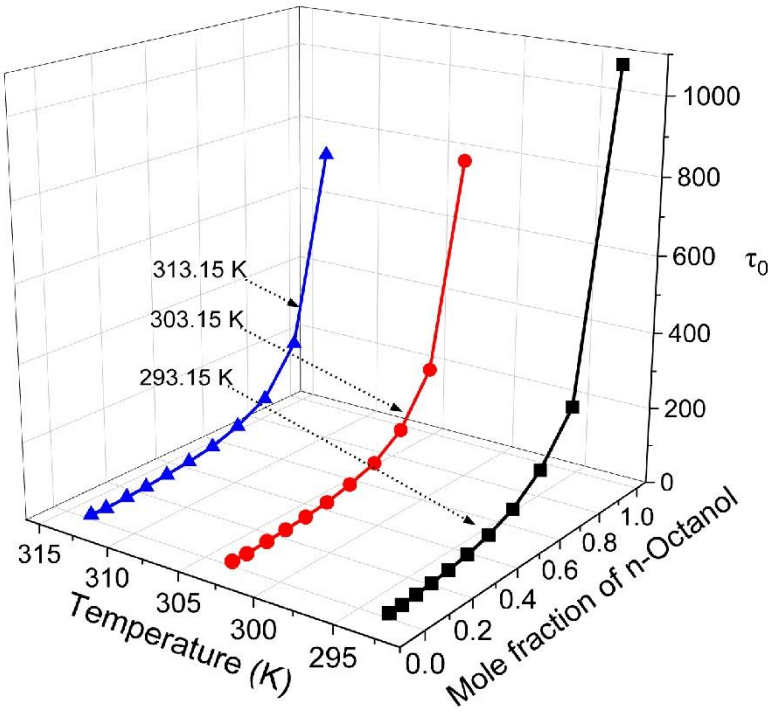

Fig.5.17 The variation of Relaxation time (τ_0) against mole fraction of n-Octanol at different temperatures.

Figure 5.17 illustrates the variation of dipolar relaxation time (τ_0) with the mole fraction of n-Octanol at different temperatures. The results indicate that τ_0 decreases with increasing temperature and further decreases with higher DMF concentrations in the mixture. Furthermore observed the relaxation time for pure n-Octanol is 769.34 ps, while for pure DMF, it is significantly lower at 12.47 ps, which is 61.69 times less at 303.15 K. As the mole fraction of n-Octanol increases, the relaxation time (τ_0) also increases. In the mole fraction range of $0.0 \leq X \leq 0.4232$, the relaxation time increases moderately with small concentration of n-Octanol molecules in the mixture. This suggests that in the DMF-rich region, the self-associated H-bonds of n-Octanol are disrupted and form new, weaker hydrogen bonds with DMF molecules. Further it has been observed that the concertation of n-Octanol increases beyond $X \geq 0.4232$, the relaxation time increases rapidly because the large number of n-Octanol molecules in the mixture preserves the self-associated hydrogen bonds of n-Octanol. This suggests that as the concentration of DMF decreases in the mixture, the relaxation behavior of n-Octanol changes, indicating hetero interactions that disrupt the existing structure.

The excess parameters with regard to static dielectric constant (ε_0) and relaxation time (τ_0) give important insights into the interaction between the polar and nonpolar liquid mixtures. These properties play a crucial role in detecting cooperative domains within

the mixture and can serve as indicators of multimer formation due to intermolecular association [51]. The excess static permittivity $(\varepsilon_0)^E$ values of the binary mixtures provide experimental evidence of the formation of complexes through H-bonds. The excess static permittivity, excess inverse relaxation time $(1/\tau)^E$ is determined through the relation (3.20) and (3.21) [52]. Figure 5.18 shows the variation of excess permittivity $(\varepsilon_0)^E$ as a function of the mole fraction of n-Octanol in DMF at different temperatures. The excess permittivity is consistently negative across the entire composition range (0.0 →1.0) at all temperatures. This suggests that the interaction between the mixture's components reduces the total number of effective dipoles, leading to the formation of multimer structures. Specifically, DMF acts as a structure breaker for n-Octanol, disrupting its hydrogen bonded network and causing neighboring dipoles to orient in opposite directions (antiparallel), thereby decreasing the number of parallel-aligned effective dipole moments. This reduction leads to the formation of multimers with lower effective dipole moments.

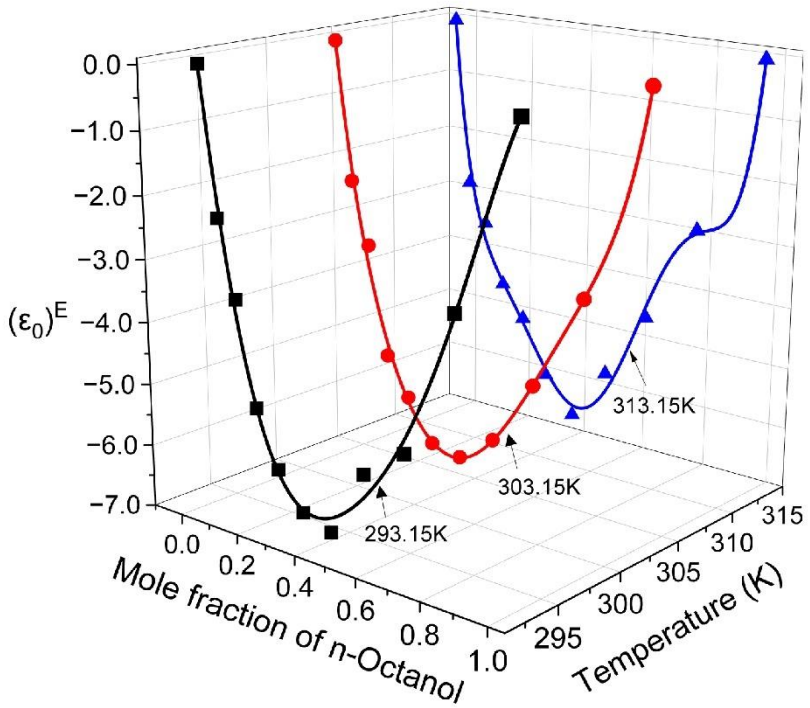

Fig. 5.18 Plot of excess dielectric constant $(\varepsilon_0)^E$ against mole fraction of n-Octanol in binary mixtures at different temperatures.

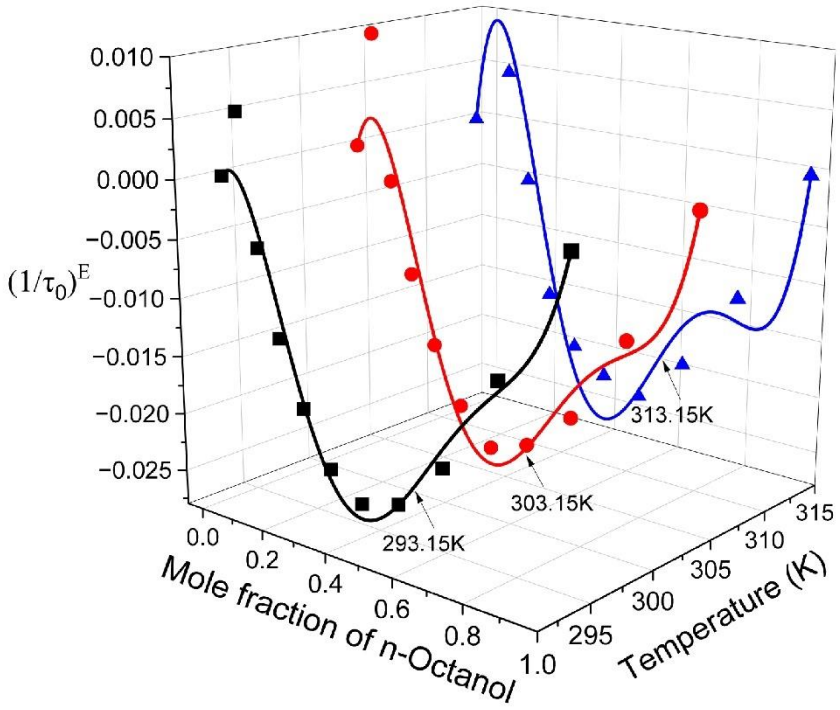

Fig. 5.19 Plot of excess inverse relaxation time $(1/\tau_0)^E$ against mole fraction of n-Octanol in binary mixtures at different temperatures.

In Fig. 5.19 the observation of all concentration (at 293.15 K) negative values for the excess inverse relaxation time $(1/\tau_0)^E$ indicates the presence of linear structures indicated by slow rotation under the influence of an external changing field. This means that addition of n-octanol to DMF induces the formation of a hindering field, resulting in a diminished rate of rotation for effective dipoles. The derived information regarding solute–solvent dynamics reveals that the addition of n-octanol impedes the rotational motion of molecules, highlighting the nuanced impact of this interaction on the rotational behavior of linear structures within the system [14].Furthermore, The data reveal that $(1/\tau_0)^E$ (at 303.15K and 313.15K) is positive at low n-Octanol concentrations (between X= 0.0 and 0.0516 mole fraction), which suggests that the dipoles rotate quickly. This fast rotation is likely due to the formation of monomeric structures that facilitate dipole movement [53,54]. The values of $(1/\tau_0)^E$ found to be negative in the mole fraction range $0.1090 \leq X \leq 1.0$ suggests that DMF and n-Octanol molecules form linear structures through intermolecular hydrogen bonding, which creates a retarding electric field and slows down the rotation of the dipoles [55,56]. The excess static dielectric constant $(\varepsilon_0)^E$ and excess inverse relaxation time $(1/\tau_0)^E$ data were fitted using the Redlich-Kister polynomial [10]. The polynomial form,

coefficients and correlation coefficient (R) and standard deviation (δ) are listed in Table 5.7.

Table 5.7 Value of coefficients of R. K. Polynomial, correlation coefficient (R) and standard deviation (δ) for excess dielectric constant $(\varepsilon_0)^E$ and excess inverse relaxation time $(1/\tau_0)^E$ at different temperatures.

Excess properties	Temp. (K)	a_0	a_1	a_2	a_3	R	δ
$(\varepsilon_0)^E$	293.15	-25.1194	11.3522	-5.9806	2.6774	0.9968	0.2337
	303.15	-24.4968	9.3123	-8.1705	-0.0360	0.9977	0.1915
	313.15	-23.4542	5.9718	-3.6246	13.4799	0.9873	0.3263
$(1/\tau_0)^E$	293.15	-0.0989	-0.0579	0.0533	-0.1526	0.9802	0.0025
	303.15	-0.0980	0.0632	0.0657	-0.2159	0.9684	0.0003
	313.15	-0.0960	0.0909	0.1042	-0.3787	0.9435	0.0053

5.3.2.3 Kirkwood correlation factor

The determined values of effective Kirkwood correlation factor (g^{eff}) and Corrective Kirkwood correlation factor (g^f) over the entire concentration range (X= 0.0 →1.0) of n-Octanol at different temperatures are reported in Table 5.8. The temperature and concentration dependence of g^{eff} and g^f for the studied system (n-Octanol + DMF) is shown in Fig. 5.20 and Fig. 5.21, respectively. The non-linear behavior observed in these mixed solvents with varying concentrations of n-Octanol corroborates changes in dipolar ordering due to weak hydrogen bond (H) between constituents' molecules of the binary mixtures. For pure n-Octanol and DMF, the values of g^{eff} are 2.72 and 1.14 (303.15 K). This indicates a strong parallel dipole ordering in n-Octanol and an antiparallel dipole ordering in DMF. The value of g^{eff} remains almost unaltered upon addition of n-Octanol into DMF until the mole fraction X reaches to 0.4232 in the mixture; Beyond X > 0.4232 a rapid increment in g^{eff} is observed. This suggests that the number of parallel-aligned dipoles increases in the mixture with an addition of n-Octanol to DMF. More parallel-aligned dipoles are compensated by the antiparallel-aligned dipoles beyond the mole fraction X= 0.4232. The variation of corrective Kirkwood correlation g^f shown in Fig. 5.21, the determined values $g^f < 1$ over the mole fraction range (0.0 < X < 1.0) suggests that the formation of hydrogen-bonded hetero

structures (multimer structures through hydrogen bonding) in the binary mixture reduces the effective dipoles of constituents liquids [57].

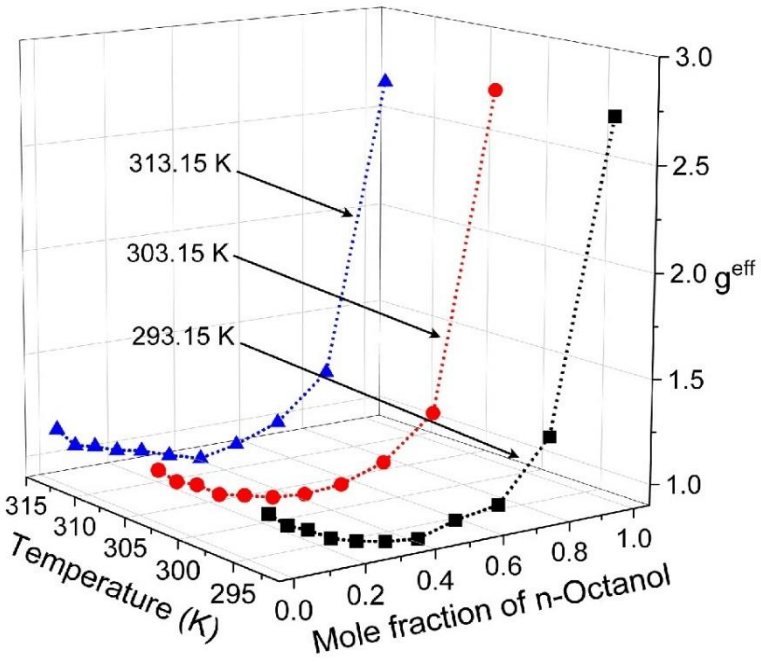

Fig. 5.20 Variation of effective Kirkwood correlation factor (g^{eff}) versus mole fraction of n-Octanol in binary mixtures at different temperatures.

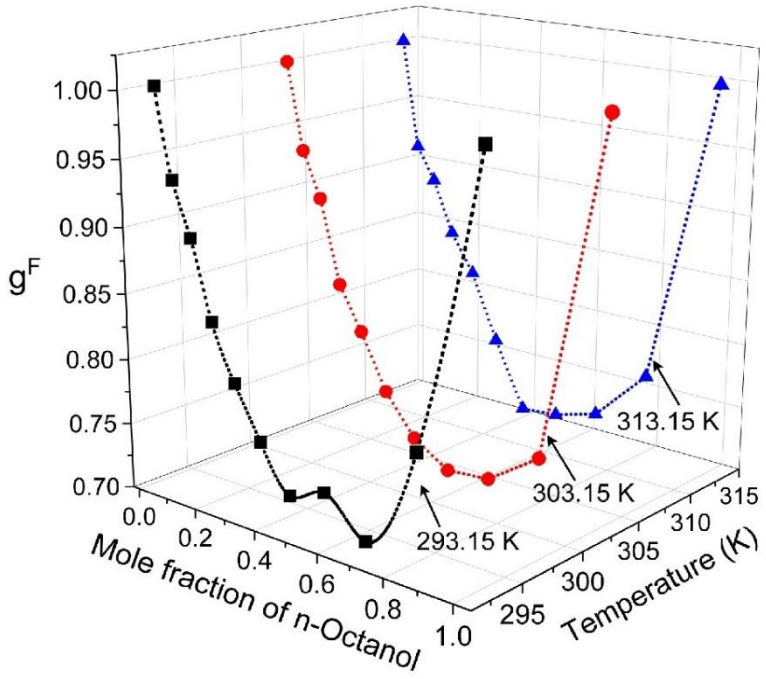

Fig. 5.21 Variation of corrective Kirkwood correlation factor (g^{f}) versus mole fraction of n-Octanol in binary mixtures at different temperatures.

Table 5.8 Determined values of effective Kirkwood correlation factor (g^{eff}) and Corrective Kirkwood correlation factor (g^{f}) of mixture of n-Octanol and DMF at different temperatures.

X_A	293.15 K	303.15 K	313.15 K
effective Kirkwood correlation factor (g^{eff})			
0.0000	1.1438	1.1493	1.1563
0.0516	1.0748	1.0795	1.0638
0.1090	1.0374	1.0476	1.0420
0.1733	0.9792	0.9819	1.0034
0.2459	0.9430	0.9552	0.9802
0.3285	0.9138	0.9208	0.9336
0.4232	0.8961	0.9065	0.8911
0.5330	0.9476	0.9203	0.9289
0.6618	0.9790	0.9899	1.0049
0.8149	1.2556	1.1885	1.2197
1.0000	2.7122	2.7213	2.6515
Corrective Kirkwood correlation factor (g^{f})			
0.0000	1.0000	1.0000	1.0000
0.0516	0.9331	0.9328	0.9140
0.1090	0.8930	0.8975	0.8881
0.1733	0.8339	0.8323	0.8466
0.2459	0.7919	0.7986	0.8164
0.3285	0.7532	0.7556	0.7640
0.4232	0.7194	0.7246	0.7114
0.5330	0.7308	0.7068	0.7140
0.6618	0.7049	0.7100	0.7238
0.8149	0.7823	0.7380	0.7654
1.0000	1.0000	1.0000	1.0000

The modified Bruggeman model provides insights into the interaction between DMF (liquid 1) and n-Octanol (liquid 2). Figure 5.22 plots the Bruggeman factor f_B against the volume fraction Φ_1 (n-Octanol) in DMF at different temperatures. Ideally, this plot should be linear according to equation 3.18 (chapter 3), but the experimental values

deviate from this linearity. To address this, the data were fitted to the modified Bruggeman equation (equation 4.7 ~ chapter 4), and the parameter "a" was determined at different temperatures. In an ideal mixture, "a" would be 1, suggesting no interaction between the component molecules. However, in this system, the value of "a" at 293.15 K, 303.15 K and 313.15 K is found to be 0.9090, 0.9157, and 0.9746 which suggests that there are molecular interactions between n-Octanol and DMF. The fact that "a" is positive but less than 1 indicates a smaller deviation from ideality and suggests that the effective volume of n-Octanol and DMF decreases upon mixing.

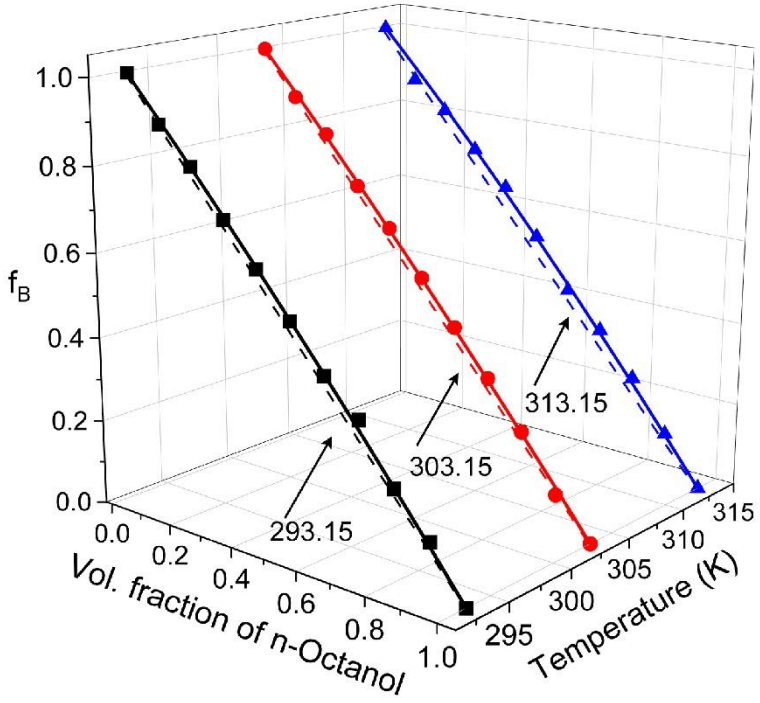

Fig. 5.22 Plot of Bruggeman factor (f_B) against vol. fraction of n-Octanol in binary mixtures at different temperatures.

5.4 Conclusion

- This study delves into the dielectric and electrical properties of binary mixtures of n-Octanol and DMF at three different temperatures (293.15 K to 313.15 K) across a frequency range of 20 Hz to 2 MHz.
- The lower frequency complex dielectric behavior is mainly governed by ionic conduction and electrode polarization phenomena. Knowledge of temperature and concentration is observed in the ionic conduction and electrode polarization processes within the n-Octanol+DMF binary mixture.
- Strong concentration dependence of DMF is evident in the electrode polarization relaxation time and ionic conductivity relaxation time.

- The experimental complex permittivity values align well with the Cole-Cole model.
- Calculated Electrode polarization relaxation time (τ_{EP}), relaxation time (τ_{EP}') and ionic relaxation time ($\tau\sigma$) using various formalisms to demonstrate good agreement.
- The study reveals dispersions in M' spectra and Z" versus Z' plots, highlighting the separation of bulk and electrode surface effects.
- Impedance data fitting with a three-element equivalent RC circuit confirms various electrical processes in the bulk sample and at the electrode surface.
- The observed perfect scaling in tan δ, M" with concentration variation indicates potential for tuning the electrical and dielectric properties of n-Octanol through mixing with DMF.
- The concentration-dependent dielectric properties (CPS ~ ε' & ε'') of n-Octanol and DMF in the microwave frequency range from 200 MHz to 20 GHz (using VNA) at a different temperature.
- The complex permittivity spectra for all binary mixtures of n-Octanol and DMF were well-fitted to the Cole-Cole dielectric model. The variations of dielectric relaxation parameters revealed a decrease in the dielectric strength ($\Delta\varepsilon$) as the concentration of n-Octanol increase suggests weak intermolecular interaction among the molecular species (n-Octanol and DMF), likely due to a reduction in dipole-dipole interactions.
- The negative values of excess static permittivity ($(\varepsilon_0)^E$) and excess inverse relaxation time ($(1/\tau_0)^E$) observed at most concentrations indicate dipole-dipole cancellation or the formation of multimers between n-Octanol and DMF molecules.
- The effective Kirkwood correlation factor suggests an increase in antiparallel dipole structures over parallel-oriented ones with increasing n-Octanol concentration in the mixture. The corrected Kirkwood correlation factor indicates that H-bonded heterostructures form in the binary mixture, leading to a reduction in the effective dipole moment compared to the pure liquids.

References

[1] L. Cai, Y. Uygun, C. Togbe, H. Pitsch, H. Olivier, P. Dagaut, S. M. Sarathy, An experimental and modeling study of n-octanol combustion. Proc. Combust. Inst. 35, (2015) 419-427.

[2] J. Julis and W. Leitner, Synthesis of 1-Octanol and 1,1-Dioctyl Ether from Biomass-Derived Platform Chemicals, Angew. Chem. Int. Ed. 51, (2012) 1-6.

[3] P. Petong, R. Pottel, U. Kaatze, Dielectric relaxation of H-bonded liquids. Mixtures of ethanol and n-hexanol at different compositions and temperatures, J. Phys. Chem. A. 103 (1999) 6114–6121.

[4] U. Kaatze, Microwave dielectric properties of liquids, Radiat. Phys. Chem. 45 (1995) 549–566.

[5] S. Schwerdtfeger, F. Köhler, R. Pottel, U. Kaatze, Dielectric relaxation of hydrogen bonded liquids: Mixtures of monohydric alcohols with n-alkanes, J. Chem. Phys. 115 (2001) 4186–4194.

[6] R. J. Sengwa, A comparative study of non-polar solvents effect on dielectric relaxation and dipole moment of binary mixtures of mono alkyl ethers of ethylene glycol and of diethylene glycol with ethyl alcohol, J. Mol. Liq. 123 (2006) 92–104.

[7] U. Kaatze, Hydrogen network fluctuations: Dielectric spectra of glycerol–ethanol mixtures, Chem. Phys. 403 (2012) 74–80.

[8] U. Kaatze, Dielectric and structural relaxation in water and some monohydric alcohols, J. Chem. Phys. 147 (2017) 24502.

[9] M.W. Sagal, Dielectric relaxation in liquid alcohols and diols, J. Chem. Phys. 36 (1962) 2437–2442.

[10] O. Redlich, A.T. Kister, Algebraic representation of thermodynamic properties and the classification of solutions, Ind. Eng. Chem. 40 (1948) 345–348.

[11] A.N. Prajapati, A.D. Vyas, V.A. Rana, S.P. Bhatnagar, Dielectric relaxation and dispersion studies of mixtures of 1-propanol and benzonitrile in pure liquid state at radio and microwave frequencies, J. Mol. Liq. 151 (2010) 12–16.

[12] D. R. Lide. CRC Handbook of Chemistry and Physics 90th Edition CD-ROM. CRC Press 2009-2010.

[13] V. D. A.G. Bruggeman, Berechnung verschiedener physikalischer Konstanten von heterogenen Substanzen. I. Dielektrizitätskonstanten und Leitfähigkeiten der Mischkörper aus isotropen Substanzen, Ann. Phys. 416 (1935) 636–664.

[14] P. Sivagurunathan, K. Dharmalingam, K. Ramachandran, B.P. Undre, P.W. Khirade, and S.C. Mehrotra, Dielectric study of methyl methacrylate-alcohol mixtures by Time Domain Refectometry at 293K. Main Group Chem. 4, 235 (2005).

[15] P. Sivagurunathan, K. Dharmalingam, K. Ramachandran, B. P. Undre, P. W. Khirade, S. C. Mehrotra, Dielectric studies on binary mixtures of ester with alcohol using time domain reflectometry, J. Mol. Liq. 133 (2007) 139-145.

[16] C. Wohlfarth, Static Dielectric Constants of Pure Liquids and Binary Liquid Mixtures, Supplement to Volume IV/17,book (2015).

[17] A. V. Navarkhele, R. S. Sakhare, S. M. Vijayendraswamy, V. V. Navarkhele, Dielectric Constant, Density, and Refractive Index in Binary Mixtures of Ethanol with N, N- dimethylformamide at 293.15 K, Russian Journal of Physical Chemistry A 96 (5) (2022) 945-953.

[18] H. N. Thorat, A. Murugkar, Thermo-acoustical properties of carbamide and N, N-dimethylformamide binary mixture at different temperatures. Indian J. Pure Appl. Phys 58 (2020) 141-146.

[19] A. N. Prajapati, S.P. Patel, V.A. Rana, Study of short range and long range molecular interactions in binary liquid mixtures of N, N-dimethylformamide (DMF) and 1-propanol, J. Mol. Liq. 354 (2022) 118832-118839.

[20] A. Serghei, M. Tress, J.R. Sangoro, F. Kremer, Electrode polarization and charge transport at solid interfaces. Phys. Rev. B 80 (18) (2009) 184301.

[21] P. B. Ishai, M. S. Talary, A. Caduff, E. Levy, Y. Feldman, Electrode polarization in dielectric measurements: a review. Meas. Sci. Tech. 24(10) (2013) 102001.

[22] D. P. Shaha, V. A. Rana and C. M. Trivedi, Orientational and dielectric behaviour of N, N-dimethylformamide in different non-polar solvents, Indian Journal of Pure & Applied Physics 56 (2018) 677-683.

[23] N. A. Chaudhary, K. N. Shah, C. R. Vaja, V. A. Rana, A. N. Prajapati, Dielectric Spectroscopy study of the binary mixtures of N-Hexanol with N, N-Dimethylformamide in the frequency range of 20 Hz to 2 MHz, Int. J. Mod. Phys. B, 2540033, 2024.

[24] R. J. Sengwa, S. Choudhary, P. Dhatarwal, Characterization of relaxation processes over static permittivity frequency regime and compliance of the Stokes-Einstein Nernst relation in propylene carbonate, J. Mol. Liq. 225 (2017) 42–49.

[25] R. J. Sengwa, S. Choudhary, P. Dhatarwal, Effect of ionic contaminants on dielectric dispersion and relaxation processes over static permittivity frequency region in neat liquid poly (ethylene glycol), J. Mol. Liq. 220 (2016) 1042–1048.

[26] S. Choudhary, P. Dhatarwal, R. J. Sengwa, Characterization of conductivity relaxation processes induced by charge dynamics and hydrogen-bond molecular interactions in binary mixtures of propylene carbonate with acetonitrile, J. Mol. Liq. 231 (2017) 491–498.

[27] R. J. Sengwa, S. Choudhary, A. Bald, Dielectric dispersion and electric relaxation processes induced by ionic conduction in formamide, 2-aminoethanol and their binary mixtures, J. Solut. Chem. 42 (2013) 1960–1975.

[28] J. Jadzyn, J. Swiergiel, On intermolecular dipolar coupling in two strongly polar liquids: dimethyl sulfoxide and acetonitrile, J. Phys. Chem. B 115 (2011) 6623–6628.

[29] J. Swiergiel, J. Jadzyn, Conductivity dynamics and static dielectric permittivity of highly conducting molecular liquids studied with impedance spectroscopy. Formamides, J. Phys. Chem. B 113 (2009) 14225–14228.

[30] S. Havriliak, S. Negami, A Complex Plane Analysis of α-Dispersions in some Polymer Systems. J. Polym. Sci., Part C: Polym. Symp. 14(1966) 99–117.

[31] H. P. Vankar, V. A. Rana, S. Dey, H. D. Patel, V. K. Jain, Molecular interaction in binary mixtures of 3-Bromoanisole and methanol: A microwave dielectric relaxation spectroscopy and molecular dynamic simulation study, Journal of Molecular Liquids 325 (2021) 115186.

[32] J.R. Macdonald, LEVM/LEVMW Manual–CNLS (Complex Nonlinear Least Squares) Immittance, Inversion, and Simulation Fitting Programs for WINDOWS and MS-DOS, 20.09. 2013, URL Www. Jrossmacdonald. Com/LEVM/LEVMMANUAL. Pdf. (n. d.)

[33] M. Wubbenhorst, J. Van Turnhout, Analysis of complex dielectric spectra. I. One dimensional derivative techniques and three-dimensional modelling, J. Non-Cryst. Solids 305 (2002) 40–49.

[34] H. P. Vankar, V. A. Rana, Electrode polarization and ionic conduction relaxation in mixtures of 3-bromoanisole and 1-propanol in the frequency range of 20 Hz to 2 MHz at different temperatures, J. Mol. Liq. 254 (2018) 216–225.

[35] V. A. Rana, K. N. Shah, H. P. Vankar, C. M. Trivedi, Dielectric spectroscopic study of the binary mixtures of amino silicone oil and methyl ethyl ketone in

the frequency range of 100 Hz to 2 MHz at 298.15 K temperature, J. Mol. Liq. 271 (2018) 686–695.

[36] R. J. Sengwa, S. Choudhary, S. Sankhla, Low frequency dielectric relaxation processes and ionic conductivity of montmorillonite clay nanoparticles colloidal suspension in poly (vinyl pyrrolidone)-ethylene glycol blends, Express Polym. Lett. 2 (2008) 800–809.

[37] R. J. Sengwa, S. Sankhla, Solvent effects on the dielectric dispersion of poly (vinyl pyrrolidone)-poly (ethylene glycol) blends, Colloid Polym. Sci. 285 (2007) 1237– 1246.

[38] J. Swiergiel, J. Jadzyn, Electric relaxational effects induced by ionic conductivity in dielectric materials, Ind. Eng. Chem. Res. 50 (2011) 11935–11941.

[39] S. Zhang, S. Dou, R. H. Colby, J. Runt, Glass transition and ionic conduction in plasticized and doped ionomers, J. Non-Cryst. Solids 351 (2005) 2825–2830.

[40] K. N. Shah, V. A. Rana, Dielectric spectroscopic study of solutions of amino silicone oil in the polar solvent mixtures of methyl ethyl ketone and methyl iso butyl ketone, J. mol. Liq. 288 (2019) 111078.

[41] S. M. Gateman, O. Gharbi, H. Gomes de Melo, K. Ngo, M. Turmine, V. Vivier, On the use of a constant phase element (CPE) in electrochemistry, Curr. Opin. Electrochem. 36 (2022) 101133.

[42] P. C. Torres, Relationship between constant-phase element (CPE) parameters and physical properties of films with a distributed resistivity, Electrochemical Acta 225 (2017) 592-604.

[43] B. Y. Chang, The Effective Capacitance of a Constant Phase Element with Resistors in Series, J. Electrochem. Sci. Technol., 13(4) (2022) 479-485.

[44] V. A. Rana, T. R. Pandit, Dielectric spectroscopic and molecular dynamic study of aqueous solutions of paracetamol, Journal of Molecular Liquids 290 (2019) 111203.

[45] B. A. Yezer, A. S. Khair, P. J. Sides, D. C. Prieve, Use of electrochemical impedance spectroscopy to determine double-layer capacitance in doped nonpolar liquids, J. Colloid Interface Sci. 449 (2015) 2–12.

[46] R. J. Klein, S. Zhang, S. Dou, B. H. Jones, R. H. Colby, J. Runt, Modeling electrode polarization in dielectric spectroscopy: Ion mobility and mobile ion

concentration of single-ion polymer electrolytes, J. Chem. Phys. 124 (2006)144903.

[47] V.A. Rana, T.R. Pandit, Microwave dielectric relaxation spectroscopy of paracetamol and its aqueous solutions, J. Mol. Liq. 314 (2020) 113673.

[48] A. Mohan, M. Malathi, Dielectric Relaxation and Thermodynamic Studies of Binary Mixtures of 2-Nitrotoluene with Primary and Secondary Alcohols at Different Temperatures, J. Solution Chem. 47 (2018) 667–683.

[49] S. S. Birajdar, A.C. Kumbharkhane, S.N. Hallale, P.G. Hudge, and D.B. Suryawanshi, Thermodynamic and dielectric properties of cyclohexanol-xylene binary mixtures using dielectric spectroscopy. Polycycl. Aromat. Compd. 43, 1619 (2023).

[50] S. Jana, S. Garain, S. Sen, and D. Mandal, The infuence of hydrogen bonding on the dielectric constant and the piezoelectric energy harvesting performance of hydrated metal salt mediated PVDF films. Phys. Chem. Chem. Phys. 17, 17429 (2015).

[51] S.P. Patel, A.N. Prajapati, H.P. Vankar, and V.A. Rana, Dielectric dispersion response of binary mixtures of n-butanol and valeronitrile. Adva. Mat. Rese. 1169, 73 (2022).

[52] R.J. Sengwa, V. Khatri, S. Sankhla, Dielectric behaviour and hydrogen bond molecular interaction study of formamide-dipolar solvents binary mixtures, J. Mol. Liq. 144 (2009) 89–96.

[53] R.J. Sengwa, S. Sankhla, Characterization of heterogeneous interaction in binary mixtures of ethylene glycol oligomer with water, ethyl alcohol and dioxane by dielectric analysis, J. Mol. Liq. 130 (2007) 119–131.

[54] G. Ravi, P.B. Undre, K. Ramachandran, K. Samuvel, Dielectric relaxation study of amides with alcohol mixtures by time domain reflectometry, South African J. Chem. Eng. 24 (2017) 71–81.

[55] B.D. Achole, A. V. Patil, V.P. Pawar, S.C. Mehrotra, Study of interaction through dielectrics: Behavior of - OH group molecules from 10 MHz to 20 GHz, J. Mol. Liq. 159 (2011) 152–156.

[56] R.J. Sengwa, S. Sankhla, V. Khatri, Dielectric characterization and molecular interaction behaviour in binary mixtures of amides with dimethylsulphoxide and 1, 4-dioxane, J. Mol. Liq. 151 (2010) 17–22.

[57] V. A. Rana, H. P. Vankar, H.A. Chaube, Static Permittivity and Refractive Index of Binary Mixtures of 3-Bromoanisole and 1-Propanol at Different Temperatures, J. Chem. Eng. Data 60 (2015) 3113-3119.